SYSTEMS, SCIENCE AND SOFTWARE

SSS-R-75-2684

12

SENSITIVITY ANALYSIS OF A CHEMICAL LASER SYSTEM

Final Report

Sponsored by

Advanced Research Projects Agency
ARPA Order No. 1806
Program Code No. 5E20

Contract No.: N00014-75-C-0981
Effective Date of Contract: 21 March 1975
Contract Expiration Date: 30 June 1975
Amount of Contract: $19,367

Principal Investigator: Dr. Howard B. Levine (714) 453-0060
Scientific Officer: Dr. J. G. Dardis

The views and conclusions contained in this document are those of the authors and should not be interpreted as necessarily representing the official policies, either expressed or implied, of the Advanced Research Projects Agency or the U. S. Government.

August 1975

P O BOX 1620, LA JOLLA, CALIFORNIA 92037, TELEPHONE (714) 453-0060

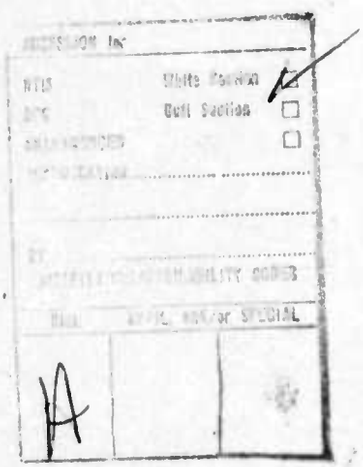
NTIS
DTIC
Buff Section
DIST
A

SYSTEMS, SCIENCE AND SOFTWARE

SSS-R-75-2684

SENSITIVITY ANALYSIS OF A CHEMICAL LASER SYSTEM

Final Report

Sponsored by

Advanced Research Projects Agency
ARPA Order No. 1806
Program Code No. 5E20

Contract No.: N00014-75-C-0981
Effective Date of Contract: 21 March 1975
Contract Expiration Date: 30 June 1975
Amount of Contract: $19,367

Principal Investigator: Dr. Howard B. Levine (714) 453-0060
Scientific Officer: Dr. J. G. Dardis

August 1975

P.O. BOX 1620, LA JOLLA, CALIFORNIA 92037, TELEPHONE (714) 453-0060

UNCLASSIFIED

SECURITY CLASSIFICATION OF THIS PAGE (When Data Entered)

REPORT DOCUMENTATION PAGE

READ INSTRUCTIONS BEFORE COMPLETING FORM

1. REPORT NUMBER

2. GOVT ACCESSION NO.

3. RECIPIENT'S CATALOG NUMBER

4. TITLE (and Subtitle)

(6) Sensitivity Analysis of a Chemical Laser System,

5. TYPE OF REPORT & PERIOD COVERED

Final Report
3/21/75 - 6/30/75

6. PERFORMING ORG. REPORT NUMBER

(14) SSS-R-75-2684

7. AUTHOR(s)

(10) H. B. Levine

8. CONTRACT OR GRANT NUMBER(s)

(15) N00014-75-C-0981,
ARPA Order-1806

9. PERFORMING ORGANIZATION NAME AND ADDRESS

Systems, Science and Software
P. O. Box 1620
La Jolla, California 92038

10. PROGRAM ELEMENT, PROJECT, TASK AREA & WORK UNIT NUMBERS

Order No. 1806
Code No. 5[illegible]0

11. CONTROLLING OFFICE NAME AND ADDRESS

Advanced Research Projects Agency
1400 Wilson Boulevard
Arlington, Virginia 22209

12. REPORT DATE

(11) August 1975

13. NUMBER OF PAGES

65 (12) 68 p.

14. MONITORING AGENCY NAME & ADDRESS (if different from Controlling Office)

15. SECURITY CLASS. (of this report)

Unclassified

15a. DECLASSIFICATION/DOWNGRADING SCHEDULE

16. DISTRIBUTION STATEMENT (of this Report)

(9) Final rept. 21 Mar - 30 Jun 75,

17. DISTRIBUTION STATEMENT (of the abstract entered in Block 20, if different from Report)

Approved for public release; distribution unlimited.

18. SUPPLEMENTARY NOTES

19. KEY WORDS (Continue on reverse side if necessary and identify by block number)

Chemical laser, laser, reaction kinetics, kinetics, chemical kinetics, hydrogen fluoride, sensitivity, sensitivity analysis, transition probability, rate constant, rate constant uncertainty, Fourier analysis, sample, nonrandom sample

20. ABSTRACT (Continue on reverse side if necessary and identify by block number)

A new technique of sensitivity analysis has been applied to the Kerber-Emanuel-Whittier model of a pulse mode hydrogen fluoride chemical laser, so as to determine which parameter uncertainties most critically influence the model's ability to predict laser performance. The particular parameters directly considered were thirteen rate constants out of a set of 68 rate constants in the model, and also the initial concentration of fluorine atoms that start the chain processes which lead to population inversion. In an indirect sense, all 68 rate constants have been studied, because of empirical relations between

DD FORM 1 JAN 73 1473 EDITION OF 1 NOV 65 IS OBSOLETE

UNCLASSIFIED

SECURITY CLASSIFICATION OF THIS PAGE (When Data Entered)

DN 388 507

No. 20 (continued)

various sets of constants controlling the formation rates of the excited vibrational states of the hydrogen fluoride molecule.

The study covers the time period from 0.1 to 4.0 microseconds following initiation, and presently considers only zero power operation. Future work will treat the finite power case. The study demonstrates how the parameter uncertainties influence the predictions of the model. It shows that only a small subset, four in number, of all the parameters, have uncertainties which cause significant variance in the predictions. That is to say, the performance of the system, in the time range studied, is almost totally independent of the uncertainties in most of the rate constants. Most prominent at early times (0.1 μsec to 1.0 μsec) are the influences of the chain processes $H + F_2 \rightarrow HF(v) + F$ and $F + H_2(0) \rightarrow HF(v) + H$. Most prominent at later times ($\gtrsim$ 1 μsec) is the influence of the VT transfer processes $HF(v) + HF(v') \rightarrow HF(v-1) + HF(v')$. The initial concentration of F atoms, as generated by flashlamp discharge, is also found to be an important parameter of the system, both at early times ($\lesssim$ 1 μsec) and again at later times ($\gtrsim$ 3 μsec).

An interesting point arises from specific consideration of the gain on the HF (v = 4→3) transition, which is found computationally to be much smaller than the gain on the adjacent transitions HF (v = 5→4) and HF (v = 3→2). This gain is found to have a parameter dependence somewhat different from the gains between other levels. This different dependence can be related to the fact that the temperature dependence for the rate of the process $HF(v) + H \rightarrow F + H_2(0)$ has been taken, in the model, to be drastically different for the states v = 4, 5, 6 than it is for the states v = 1, 2, 3. This suggests that the low gain computed for the HF (v = 4→3) transition is due to an improperly high value being chosen for the rate constant of this deactivation process.

It would appear from this study that the HF chemical laser at zero power can be described adequately by only three chemical reactions, within the time range 0.1 - 4.0 μsec following initiation.

ABSTRACT

A new technique of sensitivity analysis has been applied to the Kerber-Emanuel-Whittier model of a pulse mode hydrogen fluoride chemical laser, so as to determine which parameter uncertainties most critically influence the model's ability to predict laser performance. The particular parameters directly considered were thirteen rate constants out of a set of 68 rate constants in the model, and also the initial concentration of fluorine atoms that start the chain processes which lead to population inversion. In an indirect sense, all 68 rate constants have been studied, because of empirical relations between various sets of constants controlling the formation rates of the excited vibrational states of the hydrogen fluoride molecule.

The study covers the time period from 0.1 to 4.0 microseconds following initiation, and presently considers only zero power operation. Future work will treat the finite power case. The study demonstrates how the parameter uncertainties influence the predictions of the model. It shows that only a small subset, four in number, of all the parameters, have uncertainties which cause significant variance in the predictions. That is to say, the performance of the system, in the time range studied, is almost totally independent of the uncertainties in most of the rate constants. Most prominent at early times (0.1 μsec to 1.0 μsec) are the influences of the chain processes $H + F_2 \rightleftarrows HF(v) + F$ and $F + H_2(0) \rightleftarrows HF(v) + H$. Most prominent at later times ($\gtrsim$ 1 μsec) is the influence of the VT transfer process $HF(v) + HF(v') \rightleftarrows HF(v-1) + HF(v')$. The initial concentration of F atoms, as generated by flashlamp discharge, is also found to be an important parameter of the system, both at early times ($\lesssim$ 1 μsec) and again at later times ($\gtrsim$ 3 μsec).

An interesting point arises from specific consideration of the gain on the HF (v = 4→3) transition, which is found computationally to be much smaller than the gain on the adjacent transitions HF (v = 5→4) and HF (v = 3→2). This gain is found to have a parameter dependence somewhat different from the gains between other levels. This different dependence can be related to the fact that the temperature dependence for the rate of the process $HF(v)+H \rightarrow F+H_2(0)$ has been taken, in the model, to be drastically different for the states v = 4, 5, 6 than it is for the states v = 1, 2, 3. This suggests that the low gain computed for the HF (v = 4→3) transition is due to an improperly high value being chosen for the rate constant of this deactivation process.

It would appear from this study that the HF chemical laser at zero power can be described adequately by only three chemical reactions, within the time range 0.1 - 4.0 μsec following initiation.

TABLE OF CONTENTS

I. INTRODUCTION

The study and analysis of chemical or other laser systems, with the purpose of developing improvements in performance, efficiency, and reliability, constitutes an important current area of applied research. An aid to and part of such research is computer simulation modeling of laser operation. Such modeling is essential for understanding of many lasers, because their complexity precludes simple analytic representation. Included among those lasers whose performance description is complex are chemical lasers. In such lasers, pumping of upper quantum levels of lasing molecules occur as a consequence of exothermic chemical reactions. Under suitable conditions this can lead to population inversion and lasing. At the same time many other chemical processes such as vibrational relaxation via VT (vibration translation) transfer work so as to degrade population inversion, and thus tend to prevent lasing. In actual operation, a laser system operates under a combination of such influences, and actual performance depends upon the subtle interplay of many effects. Understanding of laser operation calls for computer simulation study of the simultaneous interaction of numerous factors. Many such studies have been undertaken during the past several years.

A common feature of all such studies is that laser operation, and the simulation thereof, is influenced by the numerical values of many systems parameters. Some of these parameters are controllable in the sense that they may be varied ad libitum by the experimenter. Examples of such would include initial temperature and initial chemical composition of the reaction mixture (for chemical lasers), concentration of inert diluents, threshold gain, reactant flow rates (for CW chemical lasers), pumping power, system geometry and system size. Other parameters are not controllable by the

experimenter. Examples of these would be chemical reaction rates, pumping efficiency, diffusion coefficients (in flow systems), and transition probabilities of emission and absorption.

The first group of parameters discussed above differ from the second in the following respect: The first set consists of parameters which the experimenter is capable of fixing at a more-or-less precise set of values, but which he may want to study at a successive set of values which differ from one experiment to the next. The second set of parameters are constants, fixed by nature, but ones for which the true value is only imprecisely known because of limitations in, or even the complete absence of, appropriate experimental data. From a mathematical point of view, both groups of constants can be thought of as being uncertain in the sense that they are defined only to within a range of values, for one or the other of the reasons just stated.

In what may be termed the "standard" computational approach, the parameters of the first set can be adjusted to different specific values and the simulation repeated so as to study the influence of different values upon the system. In the "standard" computational approach, the parameters of the second set (exact but only imprecisely known values) are set to their most likely value. Insofar as the first set of parameters is concerned, such an approach is sufficient when the number of such parameters is small enough so that their simultaneous influences can be studied with a modest number of simulations. Insofar as the second set of parameters is concerned, typically only a few individual variations of assumed value may be studied for their possible influence upon the system.

In multiparametric systems of large size, such a standard approach may not be sufficient, in that it may not

properly uncover the possible combined simultaneous influence of changes in several parameters. What is needed then, as an adjunct to, or instead of, the standard approach, is an approach which explores, insofar as it is feasible, all of the multidimensional parameter uncertainty space of the system. On the basis of such exploration, suitably interpreted, it should then be possible to infer the influence of parametric uncertainties upon systems performance predictability.

A method of such parameter study has been developed in the past three years at Systems, Science and Software (S^3), primarily under contract sponsorship of the Defense Advanced Research Projects Agency (DARPA), as administered by the Office of Naval Research (ONR). This method has been given the acronym SAM, which stands for Sensitivity Analysis Method. It may briefly be described as an efficient computer technique for sampling multiparameter space, and for generating a collection of simulations, one for each sample in the multiparameter space. It then uses Fourier techniques to carry out an analysis of the simulations, which generates statistical mean values and standard deviations of the simulation predictions; and most importantly, generates a set of measures of the comparative importance of the various parameter uncertainties as causes of the variance in the simulation prediction.

The consequences and utility of such an analysis depends upon the outcome of each particular case. Possible examples include (1) determination of those parameters (of the second class) whose uncertainties limit prediction reliability (i.e., increase variance), so that subsequent experimentation can be directed toward developing more precise values only of such important parameters, and not of unimportant parameters; (2) determination of those "control" parameters (of the first class) which most influence system performance, so that subsequent design work may be directed toward optimization of only such critical parameters and not of noncritical parameters.

The work to be described in this report consists of an application of the SAM technique to a computer simulation model of a pulse mode hydrogen fluoride chemical laser. The work was undertaken with two principal views in mind: (1) To establish a computational capability for the application of the SAM technique to chemical lasers, an area of application of SAM not previously undertaken; (2) with respect to the hydrogen fluoride chemical laser, to seek to determine the influence of several parameter uncertainties upon laser operation, as predicted by a specific model of the laser. The parameters of primary interest were the chemical rate constants for some 68 chemical reactions which operate in this system (most of these reactions are reversible, so that effectively the number of rate constants for the system is nearly two times 68). Also studied was the influence of the initial concentration of fluorine atoms, as caused by flashlamp irradiation of the reaction mixture. This last parameter, interestingly enough, can be thought of as being partially of the first type discussed above and partially of the second type. This is because the initial concentration of fluorine atoms is proportional to flashlamp intensity, which is a controllable parameter, and also because the constant of proportionality is not precisely known, being uncertain to about a factor of two.

The results of our study, as described below, can be briefly characterized by the statement that most of the rate constant uncertainties have little effect upon the predicted behavior of the system during those regimes of its time evolution which we studied; but that a few rate constant uncertainties, specifically identified below, are critically important. The influence of initial fluorine atom concentration also is important, although not as important as some of the rate constant uncertainties. Many of our conclusions are in agreement with previous observations, which serves as a mutual reinforcement, and which demonstrates the validity and applicability of the SAM technique to chemical lasers.

The work reported herein considers the laser operating at zero power (the so-called small signal gain case). It was originally our intent to go beyond this point and deal with cases of finite laser power generation, even in this first study of chemical lasers with the SAM technique. Programming difficulties, which we now believe to be resolved, precluded us from the study of the finite power case for this report. It is our hope and expectation that we will soon be able to extend the work reported herein to the more complex mathematical environment of finite power operation.

In Section II of this report we provide a brief descriptive overview of the SAM procedure. In Section III we describe the laser model. In Section IV we describe the results of the application of the SAM technique to the model of Section III. Most of the results are presented graphically, so as to provide them in compact form*.

In Section V we interpret some of the numerical results presented in Section IV. In Section VI we discuss extension of this work both to the HF chemical laser and to other lasers, and make some concluding remarks.

---

*In the interest of conciseness, we have chosen not to present all of the results of the SAM analysis in this report, but only those which seem to be most useful or interesting. At the same time, we should indicate that all of the SAM analysis results have been permanently stored on (two) computer data tapes. Recovery of all of this data, as well as detailed interpretation thereof, could be supplied to any interested reader at a nominal processing fee. To indicate the scope of this data, the SAM method as reported here, has called for 907 successive calculations of HF chemical laser performance, for a period of 4 microseconds, with data storage at 100 nanosecond intervals of real time. Each of the 907 calculations is for a different set of systems parameters, and all of these data are now available on magnetic tape.

II. THE SAM (SENSITIVITY ANALYSIS METHOD) TECHNIQUE

The underlying key concept of this new method is a mathematical theorem first proven by Hermann Weyl.[1] This theorem considers the problem of the evaluation of a multi-dimensional integral of the form

$$\langle F \rangle \equiv \int \cdots \int F(k_1, k_2 \ldots, k_N)\, W(k_1, k_2, \ldots, k_N) \times dk_1\, dk_2 \ldots dk_N \quad , \tag{2.1}$$

where W is a statistical weighting function.

It utilizes the concept of a space filling curve, which is a curve parametrically generated by a set of equations

$$k_i = k_{i0} + G_i(\sin \omega_i s) \quad (i = 1, 2, \ldots N) \ . \tag{2.2}$$

Here k_{i0} is the midpoint of the range of k_i, and G_i is a certain transformation function such that $k_{i0} + G_i(1)$ is the upper limit of the range of k_i, and $k_{i0} + G_i(-1)$ is the lower limit of the range of k_i. The set of frequencies $\{\omega_i\}$ is incommensurate, i.e., such that the sum $\Sigma_i n_i \omega_i$ is zero for integer sets $\{n_i\}$ if and only if all n_i equal zero. Weyl demonstrated that the limit

$$L \equiv \frac{1}{2T} \lim_{T \to \infty} \int_{-T}^{T} f[k_1(s), k_2(s), \ldots, k_N(s)]\, ds \tag{2.3}$$

was identically equal to the integral $\langle F \rangle$ of Equation 2.1 for a suitable choice of the set of transformation functions $\{G_i\}$. The prescription for finding the set G_i corresponding to a

given W is explained by Cukier, et al.[2] Weyl's theorem thus converts the multidimensional integration problem of Equation 2.1 into the one-dimensional line integral problem of Equation 2.3.

The parametric curve defined by the equation set, Equation 2.2, can be termed the search curve, and the variable s can be termed the search variable. As s is varied, Equation 2.2 traces out a space filling curve in parameter space. With truly incommensurate frequencies the curve never closes upon itself, and ultimately passes arbitrarily close to any given point in parameter space. As approximated numerically on a computer, true incommensurability never holds, and the search curve takes on the appearance of a multi-dimensional Lissajous curve which ultimately closes on itself. However, a succession of approximations to incommensurate behavior can be defined which involve successively longer closed curves. Sample parameter sets can then be constructed by choosing discrete sample points along the search curve. The integration in Equation 2.3 thus is reduced to a summation over a discrete set of sample points. From this sample, it is easy to compute a mean value, such as in Equation 2.1, and also other statistical data, such as the variance of F over the sample, or even a complete histogram of the distribution of F.

Specifically, the mean value $\langle F \rangle$ of a function F for a sample of N members is given by

$$\langle F \rangle = N^{-1} \sum_{i=1}^{N} F_i \tag{2.4}$$

where the F_i are the members of the sample set. The variance σ^2 of the sample is obtained from

$$\sigma^2 = \langle F^2 \rangle - \langle F \rangle^2 \tag{2.5}$$

where

$$\langle F^2 \rangle = N^{-1} \sum_{i=1}^{N} F_i^2 \quad . \tag{2.6}$$

Other useful quantities include the standard deviation, σ, which is the square root of the variance, and the coefficient of variation, v, given by

$$v = \sigma / \langle F \rangle \quad . \tag{2.7}$$

The latter quantity is a straightforward measure of the uncertainty to be attached to the mean value, and it is the quantity that will be used to measure uncertainty in this report.

The issue of sensitivity concerns determining those directions in parameter space in which F varies most rapidly on the average. The procedure for doing this was originally developed by Cukier, et al[2] and by Schaibly and Shuler.[3] They proceeded by viewing F as a function of s (as it is, implicitly, via Equation 2.2), and by then computing the Fourier spectrum of F(s). The qualitative concept is that if F is sensitive to a particular parameter, k_j, then the Fourier spectrum of F(s) will contain a large component at the frequency ω_j at which Equation 2.2 drives the Lissajous oscillations in the k_j-direction. References 2 and 3 quantify this concept. Briefly stated, these papers consider the Fourier sine coefficients

$$B_{\omega_i} = \frac{1}{\pi} \int_{-\pi}^{\pi} F(s) \sin \omega_i \, ds \tag{2.8}$$

for the Fourier series representation of F, viewed as a function of s. They associate high (low) sensitivity with respect to a parameter k_i according as B_{ω_i} is large (small) in magnitude.

A more satisfactory interpretation of the Fourier coefficients was suggested by Levine and Schaibly[4] in a subsequent study. It is useful, for purposes of this identification to consider also the Fourier cosine coefficients

$$A_\ell = \frac{1}{\pi} \int_{-\pi}^{\pi} F(s) \cos \ell s \, ds \quad , \tag{2.9}$$

where the subscript ℓ now denotes any frequency, whether one of the fundamental set (of Equation 2.2), a harmonic thereof, or a combination frequency. It is similarly useful to consider the Fourier sine coefficients, B_ℓ, (of Equation 2.8) now for <u>all</u> frequencies and not just the fundamental set. By means of Parseval's theorem,[5] the variance of the sample, Equation 2.5, can be written as a sum-of-squares of Fourier coefficients:*

$$\sigma^2 = \frac{1}{2} \sum_{\ell=1}^{\infty} (A_\ell^2 + B_\ell^2) \quad . \tag{2.10}$$

*As written here (sum to infinity) this equation implies an infinite sample. In practice, with a finite sample, the integrals of Equations 2.8 and 2.9 are approximated by finite sums of N terms each; of these only N Fourier coefficients are linearly independent and uniquely defined, and the sum in Equation 2.10 then contains only N-1 terms, the last of which has a coefficient of 1/4 instead of 1/2. It is possible to show that this numerical Parseval's theorem holds <u>exactly</u>, in the sense that the numerical estimate of σ^2, as defined by Equations 2.4, 2.5 and 2.6 is exactly equal to the finite sum form of Equation 2.10.

This means that we can consider the ratio $(A_\ell^2 + B_\ell^2)/2\sigma^2$ to constitute the fraction of the variance of the sample which is due to oscillations at frequency ℓ. In particular, if ℓ coincides with a fundamental of Equation 2.2, or its harmonics, we can think of this ratio, evaluated for that frequency, as being the fraction of the variance due to the uncertainty in value of the corresponding parameter. That is to say, the ratio $(A_{\omega_i}^2 + B_{\omega_i}^2)/2\sigma^2$ is the fraction of the variance due to the uncertainty in parameter ω_i. An even more appropriate measure is obtained if we consider the sum of such ratios over the harmonics of each fundamental frequency

$$\frac{1}{2\sigma^2} \sum_{\ell} (A_{\ell\omega_j}^2 + B_{\ell\omega_j}^2) \quad , \tag{2.11}$$

although for some problems, including those studied in this report, most of the magnitude of the sum, Equation 2.11, occurs at the fundamental frequency.

In the language of electrical engineering, the squares of the Fourier coefficient $A_\ell^2 + B_\ell^2$, are spoken of as the AC-power spectrum of an electrical signal.[6] In electrical engineering, the power of a time varying electrical signal is decomposed by frequency, the zero frequency (i.e., steady or average) term, $\frac{1}{2} A_0^2$ being the DC power of the signal. Thus, the interpretation suggested by Levine and Schaibly[4] is a natural one, based upon extensive past analysis of signal propagation problems.

Rather than use the term power spectrum in this report, which might cause confusion with the output power of the laser, we shall speak of the expression, Equation 2.11, as the variance spectrum of any variable we wish to analyze. A principal objective will be to evaluate and interpret this variance spectrum for quantities of interest in hydrogen

fluoride chemical laser simulation models. We finally comment that although in principal the sum of harmonics indicated in Equation 2.11 should be formed, we in fact only computed the fundamental frequency terms ($\ell = 1$) in the work reported here. We have, however, been able to establish numerically that for the HF laser problem as studied here, almost all of variance appears at the fundamental frequencies, so that little error has been made in ignoring the harmonics.*

*It would not be difficult to recalculate the variance spectra, including harmonics, but again, for the specific problem of this report, no useful purpose would be served thereby.

III. HF CHEMICAL LASER MODEL

The chemical laser model studied for this report was developed and published by Kerber, Emanuel, and Whittier.[7] The model deals with a laser operating in pulsed mode. A similar system, operating CW, has also been studied by Emanuel, Cohen and Jacobs.[8] The model, in its pulse mode form, considers a laser cavity containing a spatially homogeneous gas mixture. This spatial homogenity is assumed to be maintained at all subsequent times. At the initial time (t=0) the cavity contains a gaseous mixture of hydrogen, fluorine, and an inert element, e.g., argon. Initial concentrations and temperature are specified. By means of a flashlamp discharge, a specified fraction of the fluorine molecules are assumed to be dissociated into free fluorine atoms. Chemical reactions then ensue, which because of high energy release, can lead to population inversion and lasing.

The laser cavity is assumed to be between two mirrors, one fully and one partially reflecting. The reflectivities of the two mirrors and the spacing between them fix the threshold gain, α_{th}, which determines whether or not the system lases.

In this model, as studied in References 7 and 8, the chemical evolution of the system is determined by a set of 68 reversible chemical reactions. The reaction rate constants were based upon an (unpublished) analysis by Cohen. Subsequent to the calculations by Kerber, Emanuel and Whittier, a more definitive analysis of the rate constants was reported by Cohen.[9] The former authors state that the differences between Cohen's later assessment[9] and his earlier work are not significant with respect to their HF laser model. Still later, Suchard, Kerber, Emanuel and Whittier[10] considered a similar model of a chemical laser, using a somewhat larger set of reactions, and adopting Cohen's revised rate constants.[9]

They again concluded that the revised rate constants (and also the added reactions) did not affect the predictions of the model in a significant way.

In this study, we have adopted the reactions and rate constants used by Kerber, Emanuel, and Whittier.[7] This adoption is not final, and it would be of interest to extend this work to larger and better reaction sets, as the data base improves. As indicated by Cohen,[9] this data base is now in a state of flux, so that the model adopted here is by no means final. In point of fact, a principal aim in the application of the SAM method to the HF laser problem is to help elucidate which reaction rate expressions might be unsatisfactory.

Table I lists the reactions and rate coefficients used in this study.

The equations of the model are a set of (spatially homogeneous) kinetic equations of the form

$$\frac{dN(v)}{dt} = \psi_{ch}(v) + \psi_{rad}(v,J) - \psi_{rad}(v-1,J+1) \qquad (3.1)$$

for the concentrations N(v) (units: mole cm^{-3}) of the v-th vibrational level of the HF molecule. Here $\psi_{ch}(v)$ are chemical reaction rate terms which adopt the reactions and constants of Table I. The terms $\psi_{rad}(v,J)$ and $\psi_{rad}(v-1,J+1)$ represent kinetic rates of transition into the v,J vibration-rotation level of HF, and out of this level and into the level v-1,J+1. These latter rates arise only during lasing and correspond to the rates of change in level populations due to photon-induced P-branch transitions. Emanuel has shown[11] that only the P-branch transitions are active for the HF laser.

TABLE I

REACTIONS AND RATE COEFFICIENTS*

Reaction no.	Reaction[a]	Rate coefficient[b]
1	$H_2(0) + M_2 \rightleftharpoons H + H + M_2$	$k_{-1} = 10^{18} T^{-1.0}$
2[c]	$F_2 + M_4 \rightleftharpoons F + F + M_4$	$k_2 = 5.0 \times 10^{13} e^{35.3\theta}$
3,...,6	$HF(v) + M_4 \rightleftharpoons H + F + M_4$	$k_{2+v} = 1.2 \times 10^{16} T^{-1.0} e^{135.8\theta}$ $v = 0,\ldots,3$
7	$F + H_2(0) \rightleftharpoons HF(0) + H$	$k_7 = 9.0 \times 10^{13} e^{1.6\theta}$
8	$F + H_2(0) \rightleftharpoons HF(1) + H$	$k_8 = 2k_7$
9	$F + H_2(0) \rightleftharpoons HF(2) + H$	$k_9 = 10k_7$
10	$F + H_2(0) \rightleftharpoons HF(3) + H$	$k_{10} = 5k_7$
11, 12, 13	$F + H_2(0) \rightleftharpoons HF(v) + H$	$k_{-7-v} = 10^{13} T^{0.670}$, $v = 4, 5, 6$
14	$H + F_2 \rightleftharpoons HF(0) + F$	$k_{14} = 6.0 \times 10^{13} e^{2.4\theta}$
15	$H + F_2 \rightleftharpoons HF(1) + F$	$k_{15} = k_{14}$
16	$H + F_2 \rightleftharpoons HF(2) + F$	$k_{16} = 1.5k_{14}$
17	$H + F_2 \rightleftharpoons HF(3) + F$	$k_{17} = 2.66667k_{14}$
18	$H + F_2 \rightleftharpoons HF(4) + F$	$k_{18} = 3.33333k_{14}$
19	$H + F_2 \rightleftharpoons HF(5) + F$	$k_{19} = 5.5k_{14}$
20	$H + F_2 \rightleftharpoons HF(6) + F$	$k_{20} = 5k_{14}$
21, 22	$H_2(v) + M_1 \rightleftharpoons H_2(v-1) + M_1$	$k_{20+v} = 2.5 \times 10^{-4} v T^{4.2}$ $v = 1, 2$
23,...,30	$HF(v) + M_2 \rightleftharpoons HF(v-1) + M_2$	$k_{22+v} = 9.0 \times 10^{6} v T^{1.35}$ $v = 1,\ldots,8$
31,...,38	$HF(v) + M_4 \rightleftharpoons HF(v-1) + M_4$	$k_{30+v} = 5.0 \times 10^{7} v T^{1.35} + 10^{16} v T^{-1.43}$ $v = 1,\ldots,8$
39,...,46	$HF(v) + M_5 \rightleftharpoons HF(v-1) + M_5$	$k_{38+v} = 1.3 \times 10^{-2} v T^{2.60}$ $v = 1,\ldots,8$
47,...,53	$2HF(v) \rightleftharpoons HF(v-1) + HF(v+1)$	$k_{46+v} = 4.0 \times 10^{8} T^{2.2}$ $v = 1,\ldots,7$
54,...,59	$HF(v) + HF(v+1) \rightleftharpoons HF(v-1) + HF(v+2)$	$k_{52+v} = 1.2 \times 10^{2} T^{2.80}$ $v = 1,\ldots,6$
60,...,64	$HF(v) + HF(v+2) \rightleftharpoons HF(v-1) + HF(v+3)$	$k_{58+v} = 6.0 \times 10^{-2} T^{2.90}$ $v = 1,\ldots,5$
65, 66	$HF(v) + H_2(v-1) \rightleftharpoons HF(v-1) + H_2(v)$	$k_{-64-v} = 8.0 \times 10^{5} T^{2.20}$ $v = 1, 2$
67	$HF(3) + H_2(0) \rightleftharpoons HF(2) + H_2(1)$	$k_{-67} = 1.2 \times 10^{-1} T^{2.90}$
68	$HF(2) + H_2(0) \rightleftharpoons HF(1) + H_2(1)$	$k_{-68} = 2.4 \times 10^{2} T^{2.6}$

* Catalytic species:
M_1 = H, F, Ar, HF(0),...,HF(8), 4*H_2(0), 4*H_2(1), 4*H_2(2), F_2
M_2 = 20*H, F, Ar, HF(0),...,HF(8), 2.5*H_2(0), 2.5*H_2(1), 2.5*H_2(2), F_2
M_3 = F
M_4 = H, F, Ar, HF(0),...,HF(8), H_2(0), H_2(1), H_2(2), F_2
M_5 = H, Ar, H_2(0), H_2(1), H_2(2), F_2
M_6 = HF(0),...,HF(8)

[b] The rate coefficients k_+ and k_- designate forward and backward rates, respectively, with units in terms of moles, cm³, and sec. For each reaction, the missing rate coefficient is determined from the equilibrium constant.

[c] The quantity $\theta = -(10^3/RT)$, where the temperature T is in K and R is 1.987 cal/mole-K.

* From Kerber, et al., Reference 7.

The model assumes that the rotational levels of HF are, for each vibrational quantum v, in thermal equilibrium. It also assumes lasing to occur, for fixed v→v-1, only on the J of maximum gain.

In addition to Equation 3.1, there is a set of kinetic equations for the non-lasing chemical species in the system.[7]

During lasing, adjacent (lasing) vibrational levels of HF are tied together by the approximate gain condition $\alpha=\alpha_{th}$, where the gain α is given by

$$\alpha \equiv \frac{hN_A}{4\pi}\,\omega_c(v,J)\phi(v,J)B(v,J)\left\{\frac{2J+1}{2J-1}\,N(v+1,J-1) - N(v,J)\right\} . \tag{3.2}$$

In this equation h is Planck's constant, $\phi(v,J)$ is the line profile at line center, $B(v,J)$ is the Einstein coefficient for absorption, ω_c is the wavenumber of the transition, N_A is Avogadro's number, and $N(v,J)$ is the population of the v,J rotation-vibrational level of HF. Thermal equilibrium of the rotational states implies that $N(v,J)$ satisfies

$$N(v,J) = N(v)(2J+1)\exp(-hcE_J^v/kT)/Q_r^v(T) \tag{3.3}$$

where k is Boltzmann's constant, T is the absolute temperature (assumed the same for rotation and translation) and E_J^v is the rotational energy of the v,J level, i.e., its energy relative to the v,0 level. In Equation 3.3, $Q_r^v(T)$ is the rotational partition function, i.e.,

$$Q_r^v(T) = \sum_J (2J+1)\,\exp\,(-hcE_J^v/kT) \quad . \tag{3.4}$$

The effect of the assumption Equation 3.3 upon the analysis is to reduce the number of variables in the problem considerably. Although known not to hold exactly, it is generally believed to be an excellent approximation.

For this study the line profile was assumed to be a Doppler profile. It would appear that this assumption, instead of that of the more general Voigt profile, is satisfactory.[7]

A computer program for solving the model was developed by Turner, Emanuel and Wilkins;[12] and was later improved by Emanuel, Adams and Turner.[13,14] Although the improved program was available to us, we decided not to use it, but instead to reformulate the entire program using most of the methodology of References 13 and 14, but also undertaking some changes which we hoped would cause the program to operate faster. This last point has practical merit in SAM studies because of the necessity of carrying out repetitions of the simulation in large numbers and without operator intervention to cure minor program bugs. Thus, we sought to improve efficiency and reduce computing costs.

The principal difference between our program and that of Emanuel, Adams and Turner, relates to a problem in matrix inversion which arises whenever the model is simulating lasing. Under those circumstances, it can be shown that a matrix inversion step is needed in order to determine the time derivatives of the independent vibrational population levels of HF. Emanuel, et al[12,13,14] carry out this inversion numerically. We observed while studying their work that the inversion could actually be done analytically, and we conjectured that this might lead to a faster program. We therefore decided to rewrite the program using analytic inversion, and we have in fact so done. At the present time, we are not yet sure that our analytic efforts have proved to be worthwhile; we hope to determine this in future work.

The HF chemical laser model, as described above, contains one independent variable (time) and 16 dependent variables. The latter set are the temperature, the concentrations of the nine lowest vibrational levels (v = 0 to v = 8) of HF; the concentrations of the three lowest vibrational levels (v = 0 to v = 2) of H_2; and the concentrations of F_2, F, and H. Auxiliary to these are the eight gains between adjacent vibrational levels of the HF molecule (v = 1→0 to v = 8→7), maximum J values for these gains (which latter quantities vary with time), the radiated power of each transition, the total power, the total pulse energy, and the time-to-threshold for the various lasing transitions.

The dependent variables are obtained as functions of time, by solving a set of 16 time-dependent equations for a given set of boundary conditions. The specific forms of the equations vary according to whether the various vibrational transitions are lasing or not. In the simplest case (no lasing) the 16 equations are all ordinary differential equations; in other cases, the system is a mixture of differential equations and algebraic equations of constraint. The interested reader can refer to References 12, 13 and 14 for a detailed discussion of the equations. Again, the primary difference between our numerical approach and that of Emanuel, et al.[12,13,14] is in our use of analytic rather than numerical matrix inversion.

IV. SENSITIVITY ANALYSIS OF THE HF CHEMICAL LASER: DATA

4.1 INITIAL CONDITIONS AND UNCERTAINTY RANGES

Of the sixty-eight rate constants listed in Table I, only thirteen rate constants are independent. This is because certain sets of rate constants have been assumed to be proportional to each other. For example, the seven forward rate constants for reactions 14 through 20 are so related. The basis for such assumptions are discussed by Cohen,[9] who also points out their limitations. Thus, the basic assumption of proportionality itself is only an approximation; and furthermore, the best values of the constants of proportionality are uncertain, as a consequence of experimental difficulties and ambiguities, and disagreements between the estimates of various experimenters.

The HF laser could properly be subjected to a SAM analysis of the implications of the uncertainties in the proportionality constants, and a worthwhile follow-on to this study would be such an analysis. As a preliminary, however, it seemed appropriate to us to treat the rate constants in groups, by assuming the proportionalities specified in Table I to hold as given. Our idea was that by first isolating the important reaction groups, we could later focus only on those groups within which alterations in the assumed proportionalities would have an influence. This has the practical utility of reducing the required amounts of computation by a large factor.

It then follows that the thirteen "independent" rate constants are k_{-1}, k_2, k_3, k_7, k_{-11}, k_{14}, k_{21}, k_{23}, k_{31}, k_{39}, k_{47}, k_{54}, and k_{60}, the remaining constants being determined by proportionalities.

Each of the reactions in Table I has a reverse, and therefore also a reverse rate constant. However, for a given reaction, the reverse rate constant and the forward rate

constant are uniquely interrelated via the thermodynamic equilibrium criterion, so that specifications of either rate constant fixes the specification of the other constant. The use of thermodynamic data in this regard is adequately discussed by Kerber, et al.,[7] and we followed their prescription exactly in our calculations.

In addition to the rate constants, specification of the system requires us to choose initial (t = 0) values for the species concentrations and for the temperature. We have basically followed the "standard case" described by Kerber, et al., except for the initial concentrations of fluorine species. For our study, the latter quantity is a parameter, and therefore is given a range of values. The initial concentrations and temperature are as noted in Table II for species other than for F and F_2. For the excited vibrational states of H_2 the concentrations are those for a Boltzmann distribution of H_2 molecules at 300°K. The upper level (v > 0) concentrations are so small that they have essentially no influence upon the time evolution of the system. The zero value for H is appropriate at the specified initial conditions.

The initial concentrations of the HF levels is a more interesting matter. Suchard, et al.[10] have shown experimentally that small amounts of HF can be found in H_2 - F_2 mixtures subsequent to mixing but prior to flashlamp initiation, and that these amounts increase with time. This indicates that in real experimental situations processes other than irradiation initiate reaction, and that an improvement in the modeling scheme would use nonzero HF concentrations at zero time. Suchard, et al. in fact included nonzero concentrations in their calculations.[10] As we will subsequently show (see Section V), vibrational deactivation of HF(v) by VT transfer to HF(v′) is extremely important, so that nonzero initial concentrations of HF (which would, by the way, be in thermal equilibrium over the vibrational states) would

TABLE II

INITIAL CONDITIONS

Temperature	300°K	
Species Concentrations		
Ar (inert diluent)	4.704×10^{-5}	mole cm^{-3}
H_2 (v = 0)	9.407×10^{-7}	mole cm^{-3}
H_2 (v = 1)	1.119×10^{-15}	mole cm^{-3}
H_2 (v = 2)	4.321×10^{-24}	mole cm^{-3}
H	0.	mole cm^{-3}
F	Variable, see text	
HF(v) (v = 0 to 8)	0.	mole cm^{-3}
F_2	Variable, see text	

tend to quench lasing, and might play a significant role in laser performance. This means that it would be better to use initial conditions including nonzero HF concentrations, as compared to the choice in Table II. Lack of time has precluded us from doing this as yet. It would be worthwhile to extend our work to treat the initial HF concentration as a parameter, so as to explore exhaustively its possible effect.

In the standard case of Kerber, et al.[7] the initial concentration of F_2 was taken to be 9.407×10^{-7} mole cm^{-3}; and that of F was taken to be 9.407×10^{-8} mole cm^{-3}. In applying the SAM method, with the initial F atom concentration as a parameter, it is necessary to choose a nominal or "best" value for the F atom concentration, but then to study variations about this nominal value. We originally planned to take the standard value of 9.407×10^{-8} mole cm^{-3} as our nominal value, with variations both above and below this value. Early numerical experimentation indicated to us a tendency for computing time and cost to be closely linked with the initial F atom concentration, with computing time an increasing function of the initial F atom concentration. We therefore decided, in the interest of economy, to take the nominal value of the initial F atom concentration to be one-half of the above value, i.e., we chose a nominal value of 4.704×10^{-8} mole cm^{-3}, with variations above and below this value by a factor of two. Thus, the standard case of Kerber, et al.[7] became, with respect to this one parameter, the (high) extreme case of our study.

The initial F_2 concentration was always chosen so that the sum of the concentrations of F_2 and F was equal to 1.975×10^{-6} gm atom/cm^3, which is the same as for the standard case of Kerber, et al.[7]

In summary, with respect to the initial concentrations of F and F_2, the total concentration of F (gm-atom/mole) is identical to that of Kerber, et al.,[7] but our nominal initial

concentration of free F atoms is one-half of that of their standard case.

The fourteen parameters of our study were the thirteen "independent" rate constants discussed above, plus the initial concentration of F atoms. For the rate constants, the uncertainties in their values are temperature dependent, as are the values themselves, depending in each case upon the details as to the temperatures at which experimental determinations were made. As a broad statement, the values in Table I are probably of higher reliability at temperatures near 300°K than at higher temperatures. In principle it is possible to examine by the SAM method the separate influences of uncertainties in the temperature dependence (activation energy) and the pre-exponential ("constant" or temperature independent) factor in the rate expressions. In this initial study we have not attempted this, in the interests of simplicity.

At the suggestion of N. Cohen (private communication) we have estimated the independent rate constants, as expressed in Table I, to be uncertain to a multiplicative factor of 5, independent of temperature, and with a uniform probability of occurrence in this range. That is, for each such constant k, we can write

$$\log k_0 - \log 5 \leq \log k \leq \log k_0 + \log 5 \ , \qquad (4.1)$$

where k_0 is the "nominal value", as expressed in Table I. It would be a simple matter to use other probability distributions (i.e., non-uniform) or other ranges in the SAM analysis, but past experience on kinetic problems suggests to us that our choice of a uniform distribution is adequate.

For the initial concentration of F atoms, $[F]_0$, a similar choice was made, except that the range of uncertainty is taken to be only a factor of two (G. Emanuel, private

communication), i.e.,

$$\log [F]_{0,nom} - \log 2 \leq \log [F]_0 \leq \log [F]_{0,nom} + \log 2 , \tag{4.2}$$

where $[F]_{0,nom}$ is the nominal value of $[F]_0$. This range reflects the uncertainties associated with the disassociation efficiency of the flashlamp discharge.

The preceeding part of this section defines in general terms the parameters and conditions of the laser model for which a SAM analysis was performed. Following the prescription of Cukier, et al.,[2] it was necessary, with fourteen parameters, to repetitively exercise the laser model 907 times*, each time with a different set of the fourteen parameters, as prescribed by Eq. (2.2). The frequency set employed is given by Cukier, et al. With the choice of uniform distributions, the transformation functions of Eq. (2.2) can be shown to be given by

$$G_i(x_i) = \frac{2}{\pi} \text{Arcsin } x_i , \tag{4.3}$$

where Arcsin is the principle value of the arcsin function.

The necessary 907 calculations were performed, each with the same initial conditions (except for the fluorine species, as discussed previously), and each over a real time interval of 4 microseconds. Threshold gain was chosen for this report to be large enough to suppress lasing. We hope to repeat the calculations with smaller values taken for the threshold gain. For each of the 907 calculations all dependent variables were stored at 100 nanosecond real time intervals on (two) computer tapes. (Copies of these tapes can be supplied to any interested reader at a nominal cost.) The data

*Reference 2 states that 1814 repetitions are needed, but this is in error by a factor of two. Subsequent work (Ref. 4) uncovered a symmetry in the SAM method which allows a two-fold reduction in the number of calculations.

on these tapes was subsequently subjected to SAM analysis by a second computer program designed for this specific purpose. Following debugging, the entire calculation required approximately five hours of computer time on a Univac 1108 computer.

4.2 SUMMARY OF NUMERICAL RESULTS OF SAM ANALYSIS

In this subsection, we will discuss the results of the SAM analysis by means of sixteen figures which show the results of principle interest. In particular, we will show results for the concentrations as functions of time of the six lowest vibrational states of HF (v = 0 to v = 5); and for the gains for the five transitions between these six states (v = 1→0 to v = 5→4). In carrying out the SAM analysis many other variables were also computed, and these are available on computer tape. Among the other dependent variables on the computer tapes are those listed in the previous section. Lack of time has prevented us from examining these other data as yet; we also anticipate that most of it is only of very limited interest. Detailed SAM analyses were performed on the v = 6, 7 and 8 vibrational states of HF and on the transitions v = 6→5, v = 7→6, and v = 8→7. These analyses are available, as a computer printout, in a limited supply; additional copies can be generated from the computer tape for a nominal fee. However, we have not presented the data for the higher vibrational states and gains in this report because it does not appear that lasing can occur between these states. It thus was our feeling that there would be little interest in such an analysis.

4.2.1 Concentration-Time Data

In Fig. 1 we show the concentrations as functions of time for the v = 0, v = 1, and v = 2 states of HF. In Fig. 2, the same data is shown for the v = 3, v = 4, and v = 5 states.

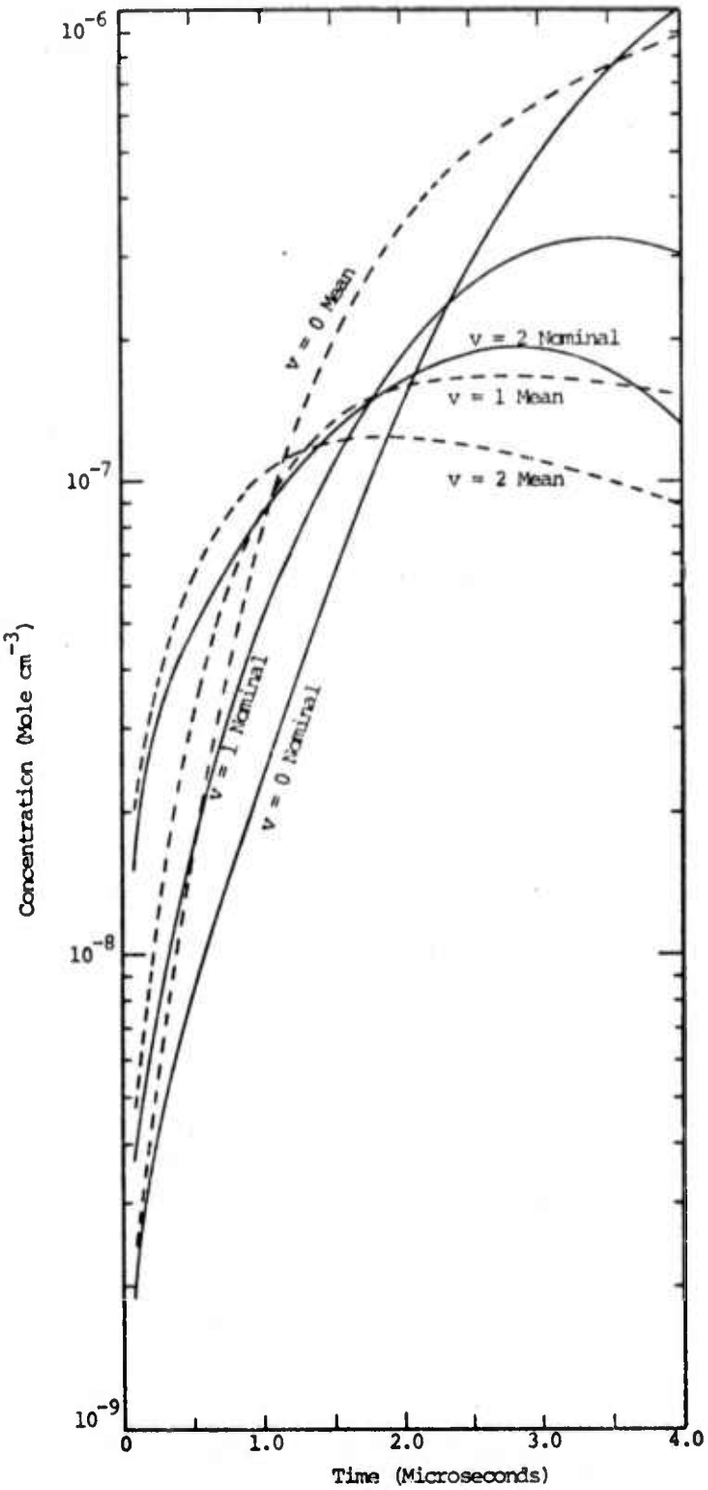

Figure 1. Concentration versus time for the v = 0, v = 1, and v = 2 vibrational states of HF. Curves show the time histories for both the nominal parameter values and for statistical mean value (average over the parameter uncertainties).

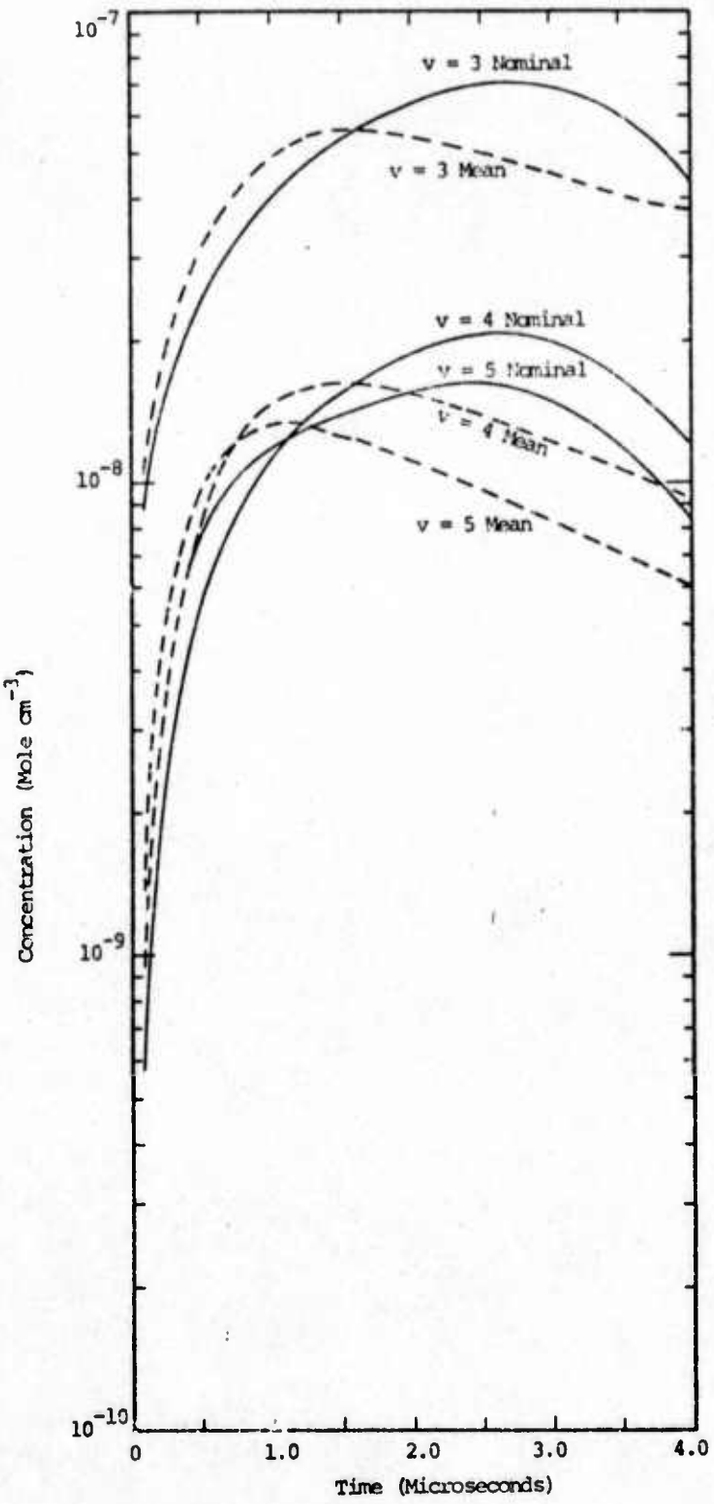

Figure 2. Concentration versus time for the v = 3, v = 4, and v = 5 vibrational states of HF. Curves show the time history for both the nominal parameter values and for the statistical mean value (average over the parameter uncertainties).

For each vibrational state, two curves are shown. The curve labeled "Nominal" gives the concentration history corresponding to the nominal parameter set. This set is made up of the thirteen independent rate constants as given in Table I, plus the "nominal" initial concentration of F atoms. The curve labeled "Mean" does not correspond to any one set of parameters. Rather, it is the average value of the concentration versus time, averaged over the set of 907 sample calculations. The curve labeled "Mean" thus is the expectation value of the concentration averaged over the (simultaneous) uncertainties of the fourteen parameters.

The Mean curve is a statistically more valid predictor than is the Nominal curve, because the former accounts for parameter uncertainties, whereas the latter does not. To the extent that the two curves disagree at a given time, we obtain a measure of the reliability of any single calculation of an excited state concentration. A glance at Figs. 1 and 2 indicates discrepancies between the two curves of as much as a factor of two. At late times there are indications that the pairs of curves are tending to come together, except for the $v = 0$ and $v = 1$ states. For the latter two states, this coming together probably commences at times beyond that for which the calculations were performed.

A tendency for each pair of curves to come together may be understood if we realize that the chemical system must eventually reach a state of equilibrium. In such a state, the uncertainties in the rate constants will no longer have an effect, since at equilibrium the chemical composition of the system becomes independent of the rate constants. On the other hand, a complete coming together cannot occur, because of the influence of the initial concentration of F atoms. In varying this initial concentration, we are also varying the internal energy of the system; because the system is a closed one (constant mass, volume, and energy), the system will attain

a final temperature which is different for different initial F atom concentrations; but then, since excited state populations are temperature dependent, there must remain some long term discrepancy between the mean and nominal curves for each vibrational state. At the 4 μsec cutoff time of our calculation, we have not yet reached the point where the discrepancy is dominated by the initial F atom concentration.

In Fig. 3, we show the zero power gains for the five transitions between the six lowest vibrational levels of HF. Again, a nominal and a mean curve are shown. For each transition, the difference between the two curves tends to be rather large; the two curves diverge from each other at late times, the Mean curves generally falling much more slowly than the Nominal curves. As we will see below, a major part of the difference can be associated with the uncertainty in the rates of the VT deactivation process $HF(v) + HF(v') \rightarrow HF(v-1) + HF(v')$, which reduce all gains and are especially influential at times $\gtrsim$ 1.0 μsec following initiation.

4.2.2 Coefficients of Variation

Better measures of the predictive uncertainties in the model than those afforded by Figs. 1-3 can be obtained. In Fig. 4 we show the coefficients of variation for the populations of the first six vibrational levels of HF; in Fig. 5 we show the coefficients of variation for the gains between these levels. It will be recalled (see Section II, Eq. 2.7) that the coefficient of variation is the ratio of the standard deviation to the mean value of a (statistically distributed) dependent variable. High reliability (small variance) corresponds to a small coefficient of variation, and vice versa. Referring to Fig. 4, we see that "coefficients of variation" for the excited state populations lie in the range 0.5 to 1.5. We can make the qualitative statement that the standard deviation thus is in each case about equal in value to the variable, i.e., it is not small.

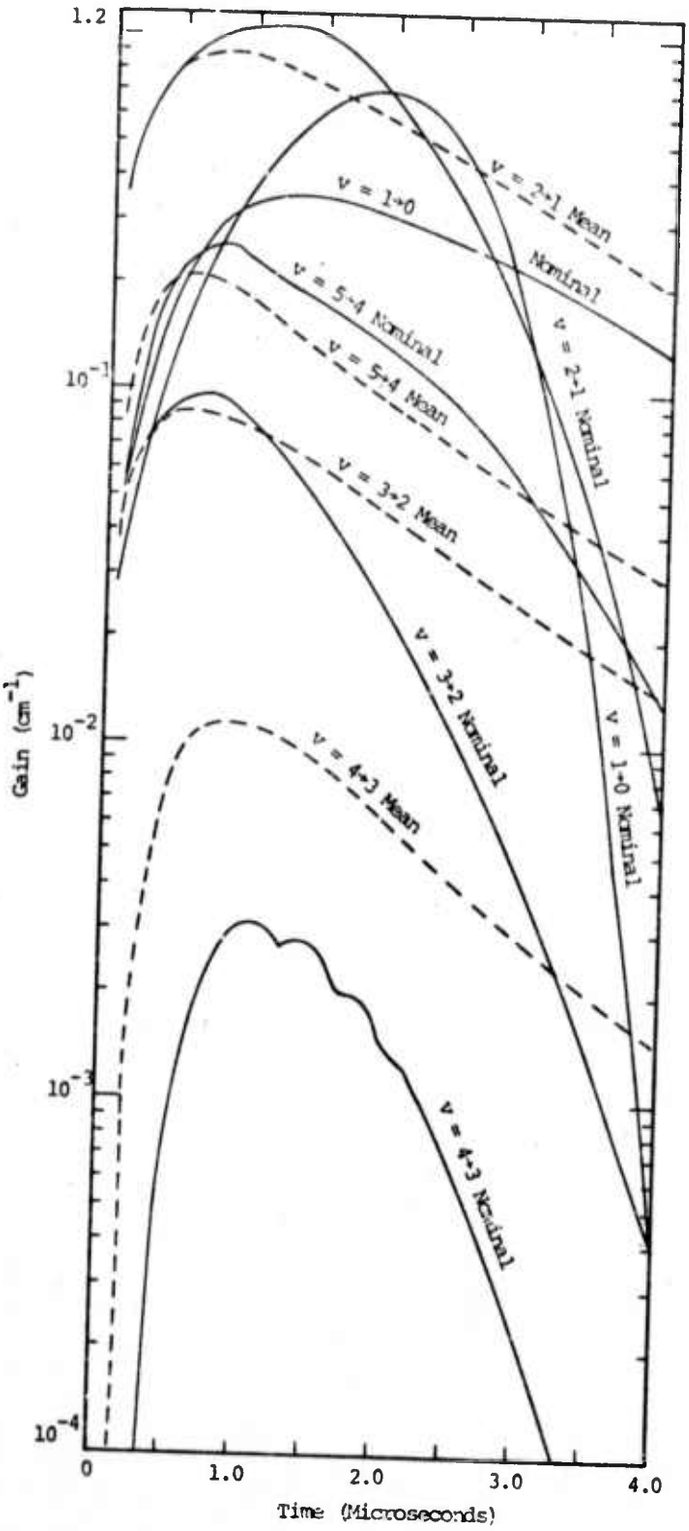

Figure 3. Zero power gains versus time for the lowest five vibrational transitions of HF. Curves show the time histories for both the nominal parameter values and for the statistical mean value (average over the parameter uncertainties).

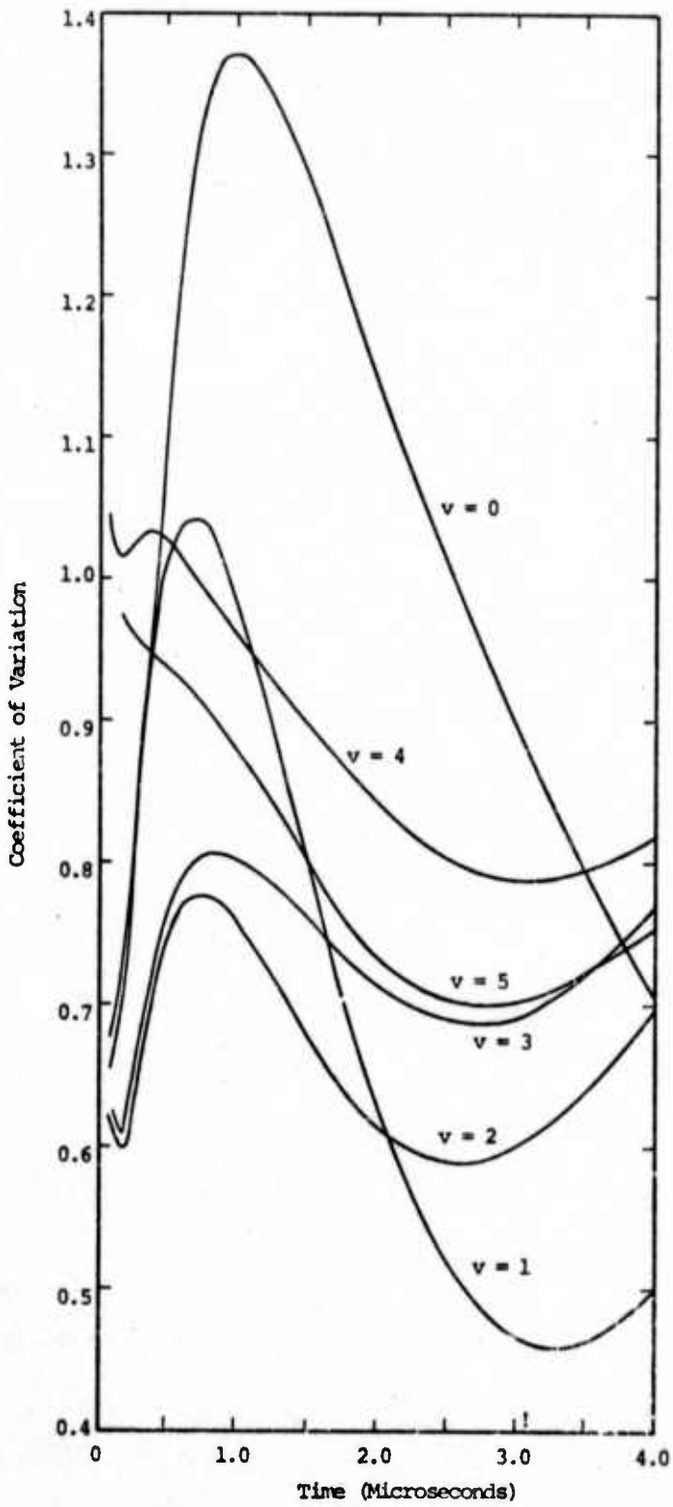

Figure 4. Coefficients of variation of the populations of the first six vibrational levels of HF, as functions of time.

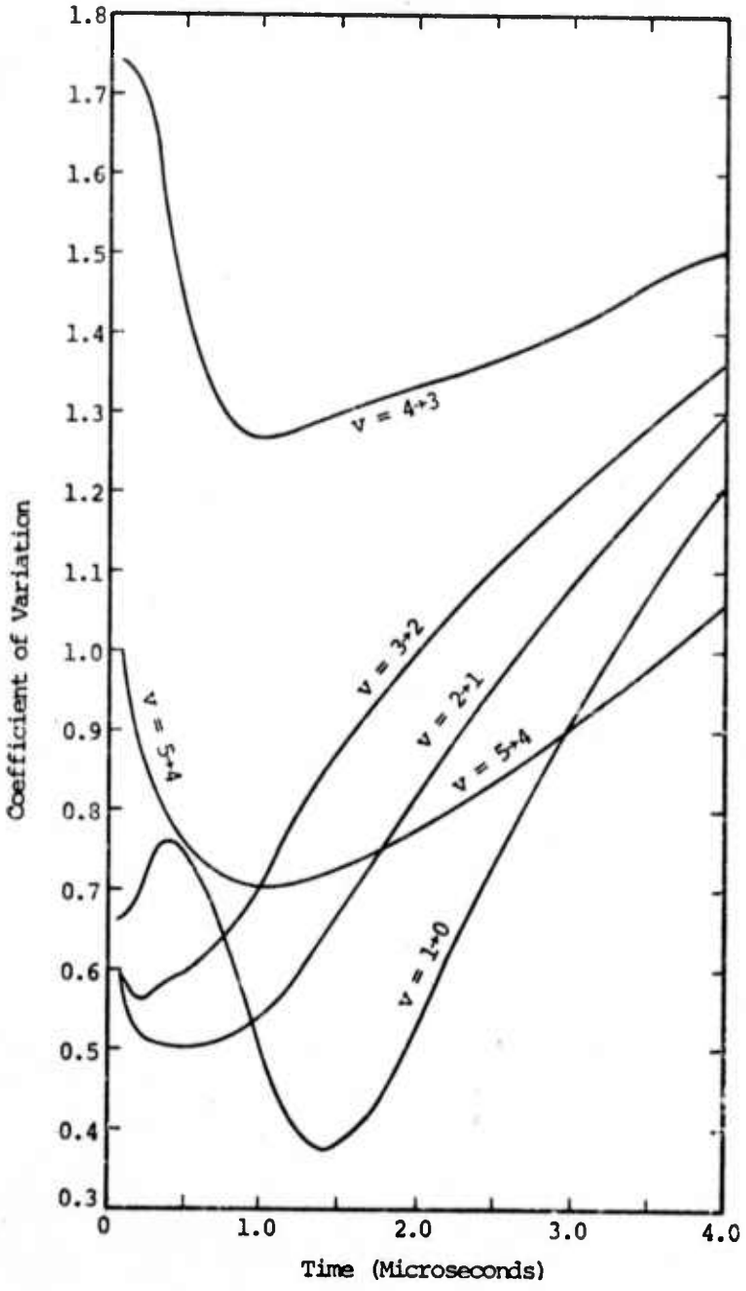

Figure 5. Coefficients of variation of the gains on the first five vibrational transitions of HF, as functions of time.

It is interesting to note that the coefficient of variation of the v = 0 level achieves a maximum at about t ≅ 1 μsec, and subsequently diminishes. This is a consequence of the approach of the system to equilibrium. In the latter state, the distribution of HF molecules among its vibrational levels will depend on the final temperature, which in turn depends upon the zero time F atom concentration, as previously noted. However, at all final temperatures achievable in our sample set of calculations, most HF molecules will end up in the v = 0 state, so that the population of this state, at equilibrium, is highly parameter insensitive. On the other hand, the excited state populations are very temperature sensitive, a fact which leads to the rising values of the corresponding coefficients of variation at long times. The oscillation of the coefficient of variation of the excited states, best exemplified by the v = 1 curve of Fig. 4 is due to the fact that different rate constants are influential in setting excited state concentrations at different times.

It is especially worth noting that the coefficients of variation of the v = 4 and v = 5 levels lie above those of other excited states; and even more noteworthy that the v = 4 curves lie above the v = 5 curve. The implication is that the v = 4 population is the least accurately predictable of all of the excited states. We will comment additionally on this below.

In Fig. 5 we show the coefficients of variation for the gains. The behavior of these curves for the v = 1→0, v = 2→1, and v = 3→2 transitions reflect the behavior of the population curves (Fig. 4) for the upper level of each transition. This is a clear indication that the gains on these transitions are dominated by the first of the two terms in the braces in Eq. 3.2.

Again worth particular note is the fact that the curve for the v = 4→3 transitions lies above all of the other curves. This fact, taken in conjunction with our previous observation on the v = 4 curve in Fig. 4, indicates that there is something "peculiar" about the model's predictions of the v = 4 level population and the v = 4→3 gain. We will discuss the peculiarity further below.

4.2.3 Variance Spectra

The data in Figs. 1-5 provide a general overview. We now turn to the variance spectra in order to determine the "causes" for the coefficients of variations, and for the discrepancies between mean and nominal predicted values, as indicated in these figures.

4.2.3.1 Variance Spectrum of the HF (v = 0) Level Population

In Fig. 6 we display the variance spectrum for the concentration versus time of the HF (v = 0) level. Of the fourteen parameters studied in our analysis, ten make negligible contributions to this variance spectrum over the time range covered (0.1 μsec to 4.0 μsec).* The curves for these ten parameters are not displayed. The remaining four parameters, k_7, k_{14}, k_{31}, and $[F]_0$ (the initial concentration of F atoms) account for nearly all of the variance. The figure shows that the relative importance of these four parameters varies with time. Thus, near t = 0.1 μsec, the uncertainty in k_7 and $[F]_0$ causes most of the variance in the model's prediction of the HF (v = 0) concentration. As time advances, these parameters diminish in relative importance, simultaneous with an increase in the importance of k_{31}, and most of all k_{14}. As we previously indicated, in the limit of infinite time,

*It is possible that at times between zero and 0.1 μsec other parameters might be significant. We hope to carry out a detailed analysis of this time range in a subsequent study.

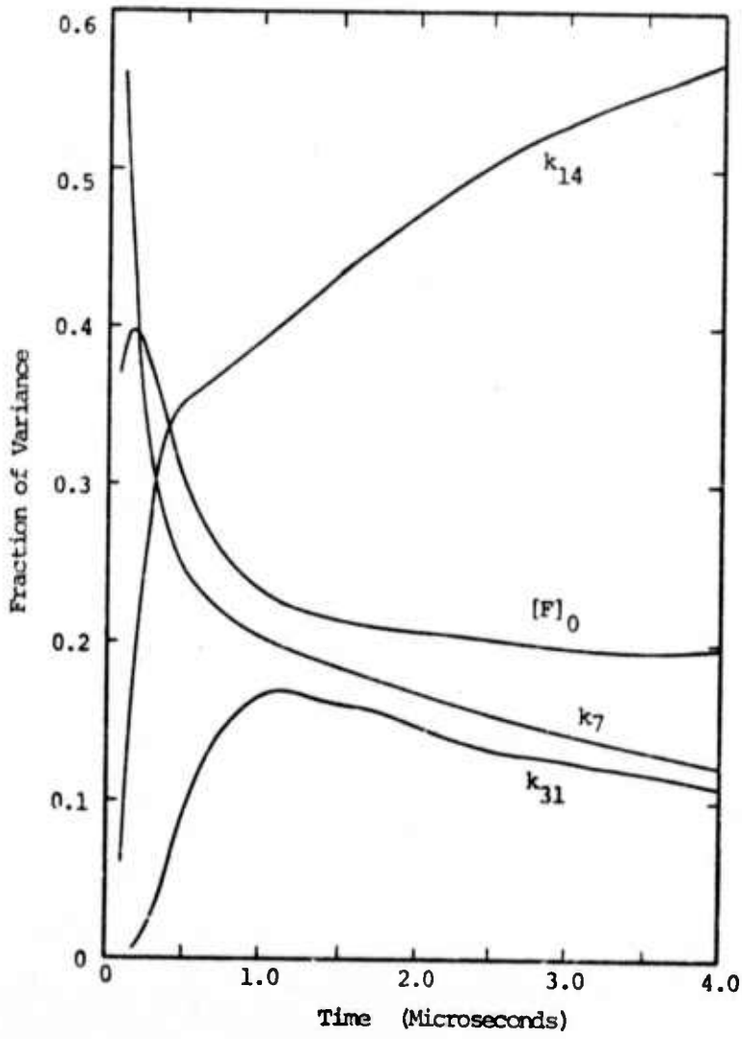

Figure 6. Variance spectrum for the population of the v = 0 vibrational level of HF.

as the system approaches equilibrium, all of the variance must become due to the uncertainty in $[F]_0$. We note in Fig. 6 that at t = 4.0 μsec, where we cut off our calculation, the contribution of $[F]_0$ has passed through a minimum and just begun to rise.

It is not difficult to rationalize the curves in Fig. 6 by referring to Table I. We see from this table that k_7 is the rate constant for the processes $F + H_2(0) \rightleftarrows HF(v) + H$ (v = 0, 1, 2, 3), and that k_{14} is the rate constant for the processes $H + F_2 \rightleftarrows HF(v) + F$ (v = 0, ..., 6). At early times, formation of HF(0) is controlled by the combined influences of $[F]_0$ and the reaction $F + H_2(0) \rightarrow HF(0) + H$. Hence the contributions of $[F]_0$ and k_7 are large. At later times, the system presumably reaches a steady state condition with respect to the reactions controlled by k_7 (in particular, reaction no. 7 of Table I), so that the rate constant uncertainty in k_7 no longer plays a role. But then reaction no. 14 becomes controlling as a production source for HF(0). To a lesser extent, reaction no. 31 (and hence k_{31}) supplies HF(0), so that the effect of uncertainty in k_{31} also becomes important. We will see below that when we come to the excited states of HF, the role of k_{31} becomes much more important.

4.2.3.2 Variance Spectrum of the HF (v = 1) Level Population

In Fig. 7 we display the variance spectrum for the concentration versus time of the HF (v = 1) level. As for the v = 0 level, only four parameters k_7, k_{14}, k_{31}, and $[F]_0$ make significant contributions to the variance between 0.1 μsec and 4.0 μsec. The curves for k_7 and $[F]_0$ again show a dominant influence for these two parameters at early times. Subsequently these curves show a monotonic decline. As previously indicated, the curve for $[F]_0$ ultimately must pass through a minimum and rise again, but evidently this minimum has not yet been achieved at 4 μsec. When we examine the curves for

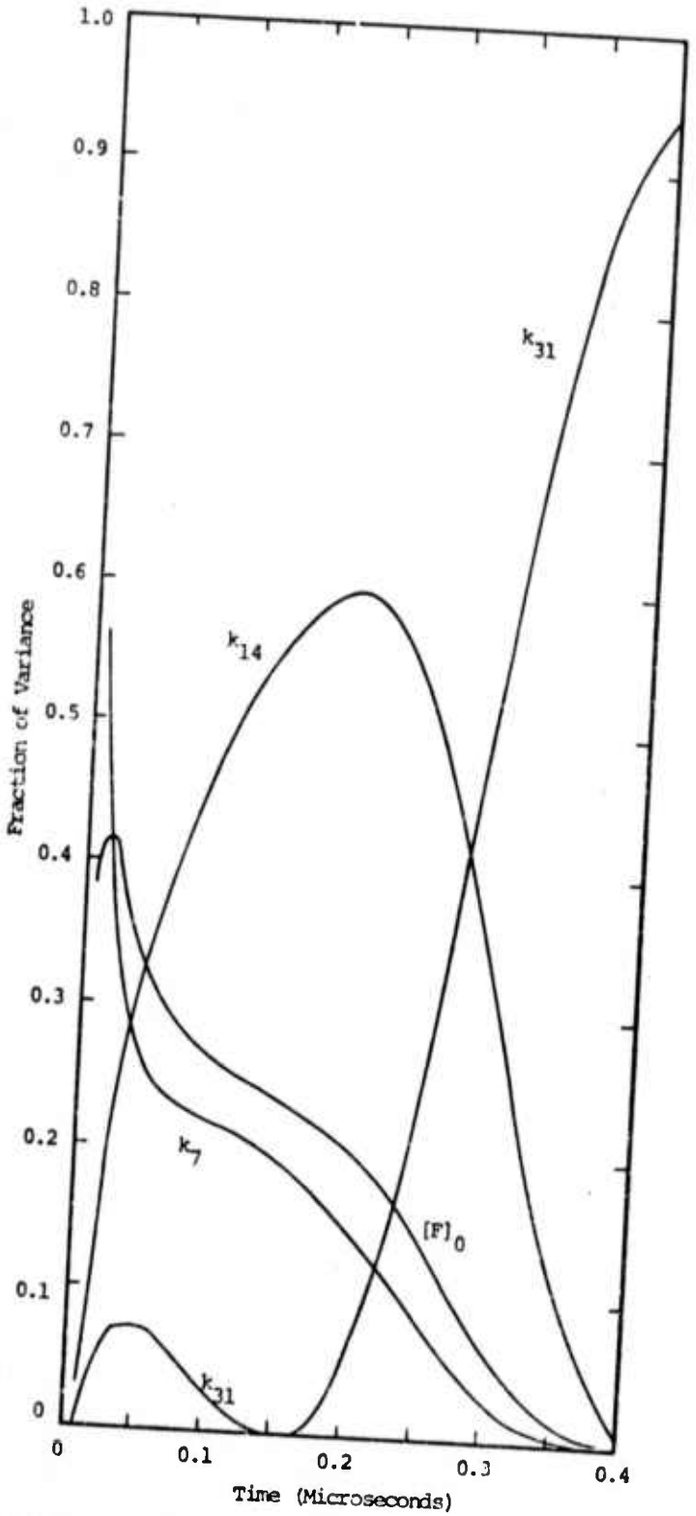

Figure 7. Variance spectrum for the population of the v = 1 vibrational level of HF.

k_{14} and k_{31}, we note some differences relative to Fig. 6. In Fig. 7, the curve for k_{14} reaches a maximum near 2.0 μsec, and subsequently declines rapidly; in Fig. 6, the maximum in the k_{14} curve (which must occur because of ultimate approach to equilibrium) has not yet appeared at 4.0 μsec. Most significantly, the curve for k_{31} in Fig. 7 rises to a very high value near 4.0 μsec, and in fact accounts for nearly all of the variance at this time. This indicates that the VT transfer process $HF(1) + HF(v') \rightleftarrows HF(0) + HF(v')$ dominates the uncertainty in the HF(1) concentration at this time. It is important to realize, by distinction, that the contribution of the VT processes of reaction no. 23 [$HF(1) + M_3 \rightleftarrows HF(0) + M_3$] and reaction no. 39 [$HF(1) + M_5 \rightleftarrows HF(0) + M_5$] to the variance is negligibly small. In these latter reactions, the species M_3 is atomic F, and the species M_5 is H + Ar + $H_2(v)$ (v = 0, 1, 2) + F_2. That is to say, lack of accurate data for k_{23} and k_{39} is not important; lack of accurate data for k_{31} is very important. This latter conclusion is dependent on several specific factors, and in particular the species concentrations. It is clear, for example, that at higher Ar concentrations than that of Table II, k_{39} could become more important.

4.2.3.3 Variance Spectrum of the HF (v = 2) Level Population

In Fig. 8 we display the variance spectrum for the concentration versus time of the HF (v = 2) level. These curves are very similar to those for the HF (v = 1) level, as shown in Fig. 7. The comments of Section 4.2.3.2 therefore also apply to these curves, with an appropriate shift in the reaction numbers (i.e., reaction no. 8 is replaced by reaction no. 9; reaction no. 15 is replaced by reaction no. 16; reaction no. 23 is replaced by reaction no. 24; reaction no. 31 is replaced by reaction no. 32; reaction no. 39 is replaced by reaction no. 40).

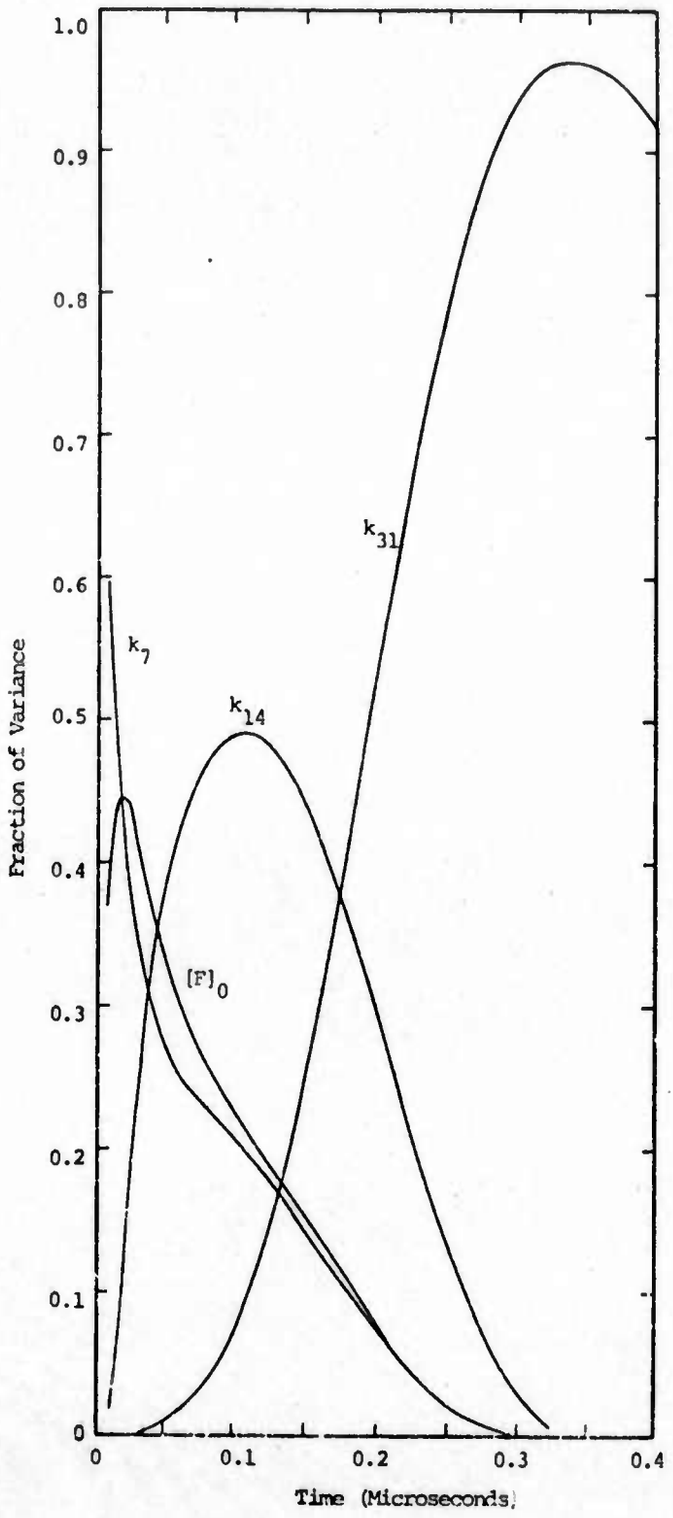

Figure 8. Variance spectrum for the population of the v = 2 vibrational level of HF.

4.2.3.4 Variance Spectrum of the HF (v = 3) Level Population

In Fig. 9 we display the variance spectrum for the concentration versus time of the HF (v = 3) level. These curves are very similar to those for the HF (v = 1) and HF (v = 2) levels, as shown in Figs. 7 and 8. The comments of Section 4.2.3.2 therefore also apply, with an appropriate shift in the reaction numbers (reaction no. 8 is replaced by reaction no. 10; reaction no. 14 is replaced by reaction no. 16; reaction no. 23 is replaced by reaction no. 25; reaction no. 31 is replaced by reaction no. 33; reaction no. 39 is replaced by reaction no. 41).

4.2.3.5 Variance Spectrum of the HF (v = 4) Level Population

When we come to the HF (v = 4) level, a new effect appears. The variance spectrum for the population of this level is shown in Fig. 10. For this level, the rate constant k_{-11} for the reaction $F + H_2(0) \rightleftarrows HF(4) + H$ makes a significant contribution to the variance. The roles of the other rate constants are similar to those for HF (v = 3) (Fig. 9), but each is shrunken in magnitude relative to this previous* figure. From Table I we see that reaction no. 11 is chemically of the same form as reaction no. 7 to 10, but that it has a drastically different temperature dependence for its rate constant. The reason for this has been discussed by Cohen.[9] The reaction of F with $H_2(0)$ is energetically inadequate to produce HF(v) for v > 3; the reaction is included in the modeling scheme, however, because the reverse process $HF(v) + H \rightarrow F + H_2(0)$ is not energetically prohibited, and it is envisioned as a possible path for deactivation of HF(v) (v > 3).

*Because the variance spectrum is defined in a normalized form (Eq. 2.11), the sum of all contributions at any given time adds up to one; hence any increase in one contribution appears at the expense of other contributions. But it should also be noted that the coefficient of variation in the HF (v = 4) level population is higher than that for the v = 1,2, or 3 levels, so that in an absolute sense the reduction in influence of the other parameters in Fig. 10 is less than a casual glance might indicate.

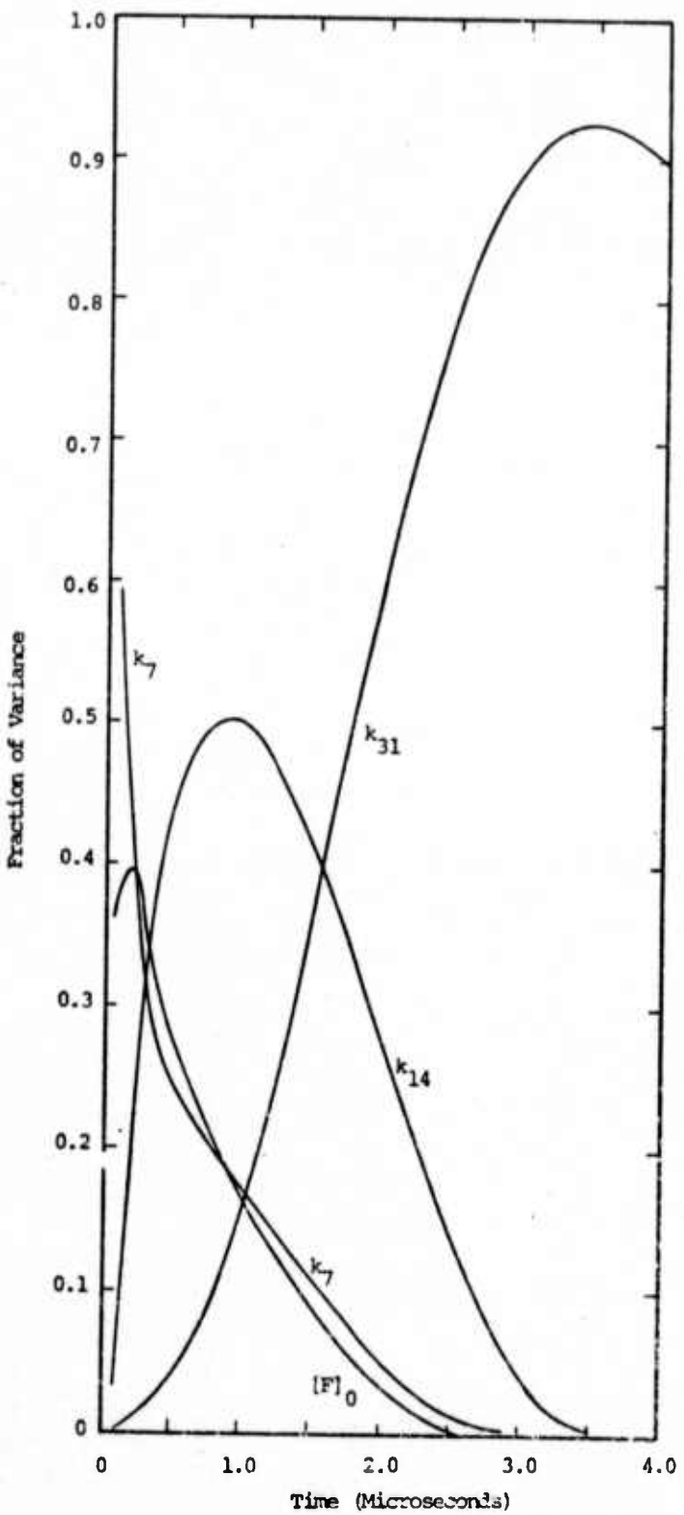

Figure 9. Variance spectrum for the population of the v = 3 vibrational level of HF.

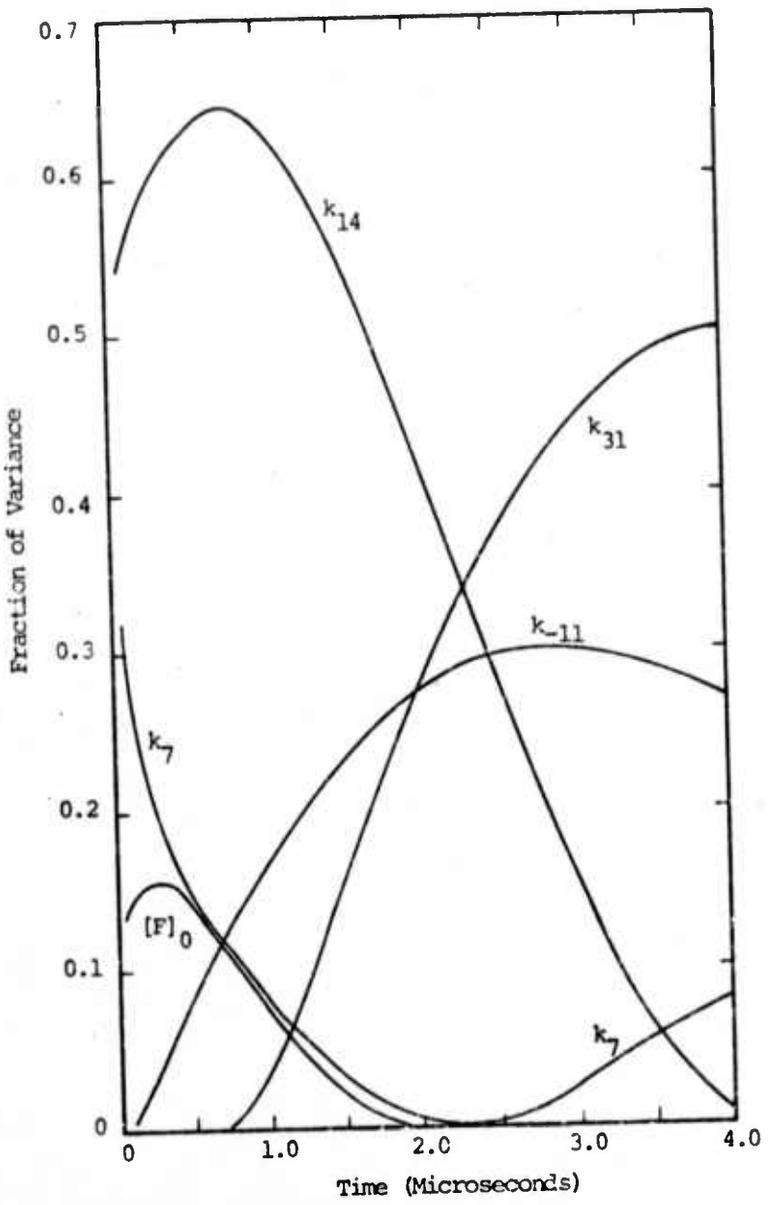

Figure 10. Variance spectrum for the population of the v = 4 vibrational level of HF.

The "sudden" appearance of the k_{-11} curve in Fig. 10, following its absence in Figs. 7, 8, and 9, is a clear indication that in this model this reverse process is indeed significant. We will discuss in Section V the question of the physical reality of this modeled effect, and in fact will argue that it is not physically reasonable.

4.2.3.6 Variance Spectrum of the HF (v = 5) Level Population

In Fig. 11 we display the variance spectrum for the concentration versus time of the HF (v = 5) level. These curves are very similar to those for the HF (v = 4) level in Fig. 10. We can anticipate therefore that conclusions concerning this level will be similar to conclusions drawn for the HF (v = 4) level. We defer further discussion to Section V.

4.2.3.7 Variance Spectrum of the Zero Power Gain on the v = 1→0 Transition of HF

The gain on any transition is functionally dependent on the populations of the two levels of the transition, and also on the temperature. We therefore expect the variance spectrum of the gain to reflect the variance spectrum of the two populations and the temperature. We have not carried out a sensitivity analysis of the temperature, although to do so would be straightforward. Brief inspection of a few of the 907 simulations done for the SAM analysis indicates that the temperature-time histories may vary by as much as a factor of two between different simulations (i.e., different parameter sets).

Turning to Fig. 12, we see displayed the variance spectrum of the HF (v = 1→0) gain as a function of time. As with the population, only a small subset of the parameters contribute significantly to the gain and only the important

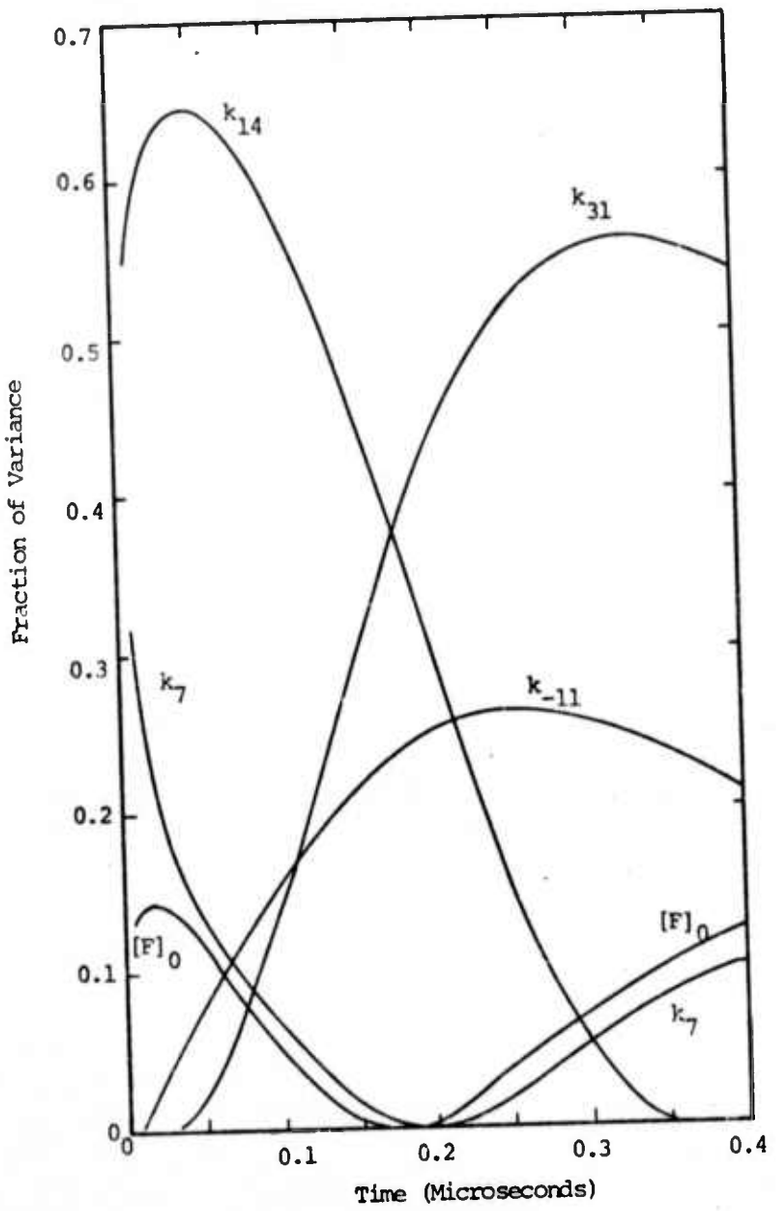

Figure 11. Variance spectrum of the population of the v = 5 vibrational level of HF.

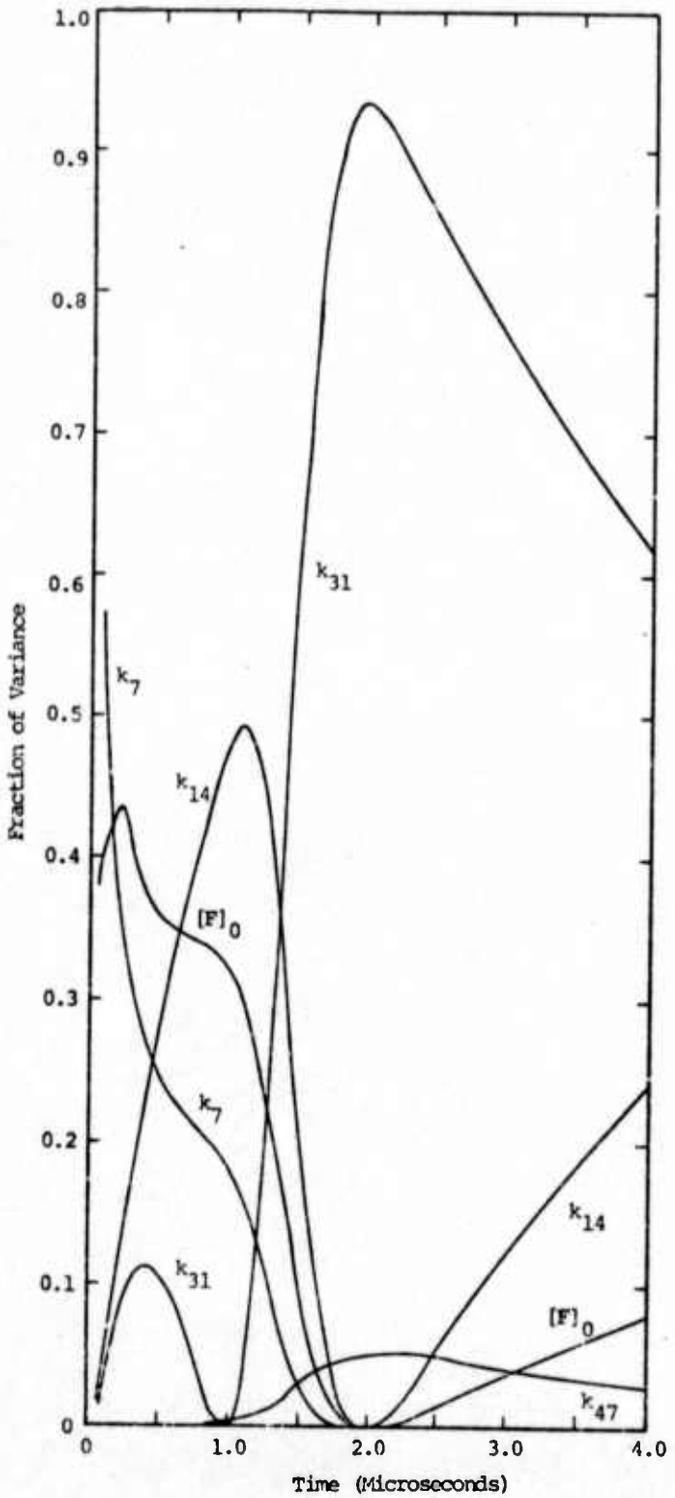

Figure 12. Variance spectrum for the zero power gain of the $v = 1 \rightarrow 0$ band of HF.

parameters are shown in the figure. In addition to the four parameters k_7, k_{14}, k_{31}, and $[F]_0$ which appear in Figs. 6 and 7, we also find in Fig. 12 a small contribution due to parameter k_{47}, which is the rate constant for the VV transfer process $2HF(1) \rightleftarrows HF(0) + HF(2)$. The timewise behavior of the other curves is similar to that seen in Figs. 6 and 7. In particular, we note that the k_{14} curve appears to be a compounding of the influences seen for the HF(0) level seen in Fig. 6 (k_{14} rising at long times) and Fig. 7 (k_{14} peaking at intermediate times).

4.2.3.8 Variance Spectrum of the Zero Power Gain on the v = 2→1 Transition of HF

In Fig. 13 we display the variance spectrum for the gain on the HF (v = 2→1) transition. Except for the facts that the small k_{47} contribution which appears in Fig. 12 does not appear in Fig. 13, and the minimum in the k_{31} curve does not occur, the curves in Fig. 13 are similar to those in Fig. 14. The comments of Section 4.2.3.7 thus also apply in this case, with a shift in reaction numbers (i.e., reaction no. 8 replaces reaction no. 7; reaction no. 9 replaces reaction no. 8; etc.).

4.2.3.9 Variance Spectrum of the Zero Power Gain on the v = 3→2 Transition of HF

In Fig. 14 we display the variance spectrum for the zero power gain on the HF (v = 3→2) transition. The curves are similar to those in Fig. 12, so that the comments of Section 4.2.3.7 also apply here, with a shift in reaction numbers (i.e., reaction no. 9 replaces reaction no. 7; reaction no. 10 replaces reaction no. 8; etc.). It should be noted that the reverse reaction k_{-11} makes a contribution to the variance spectrum shown in this figure. This occurs because this reaction populates the v = 3 state at the expense of the v = 4 state, as will become apparent in the next subsection.

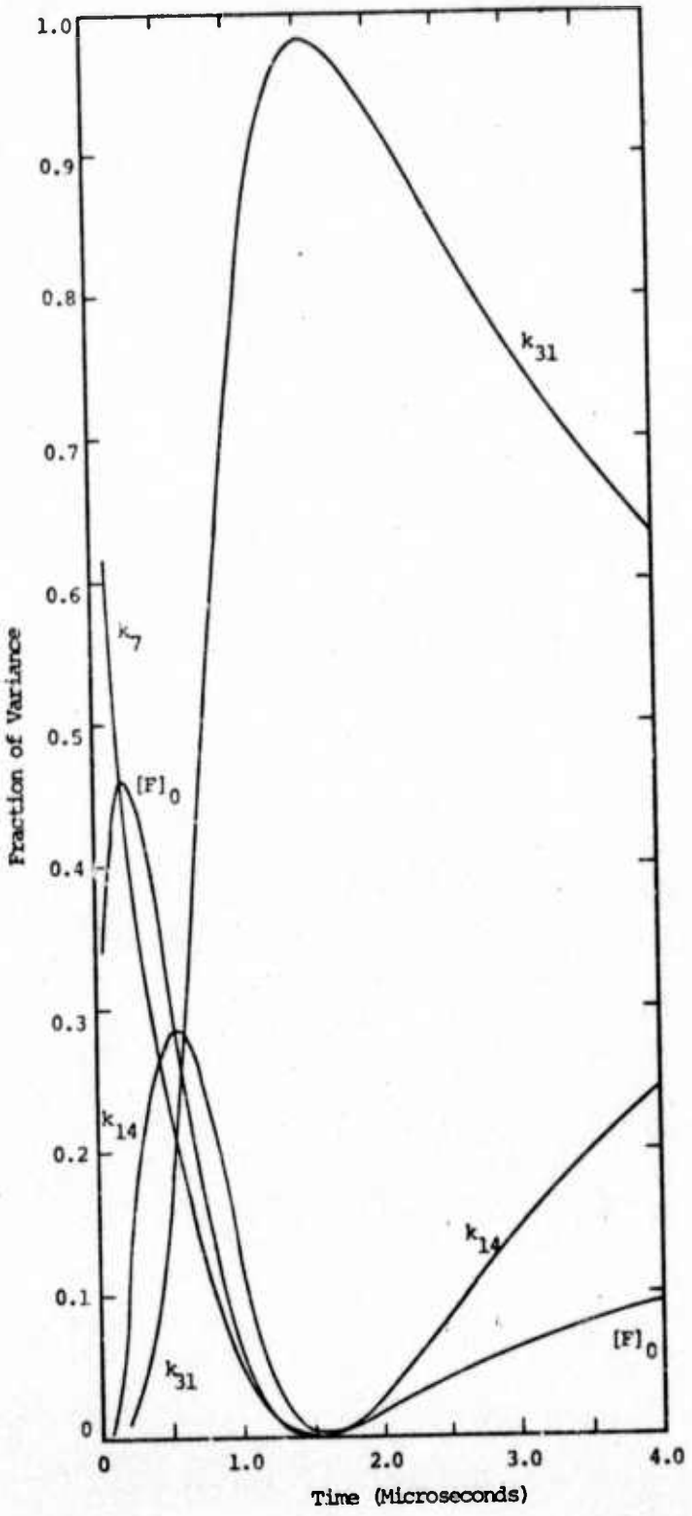

Figure 13. Variance spectrum for the zero power gain of the v = 2 → 1 band of HF.

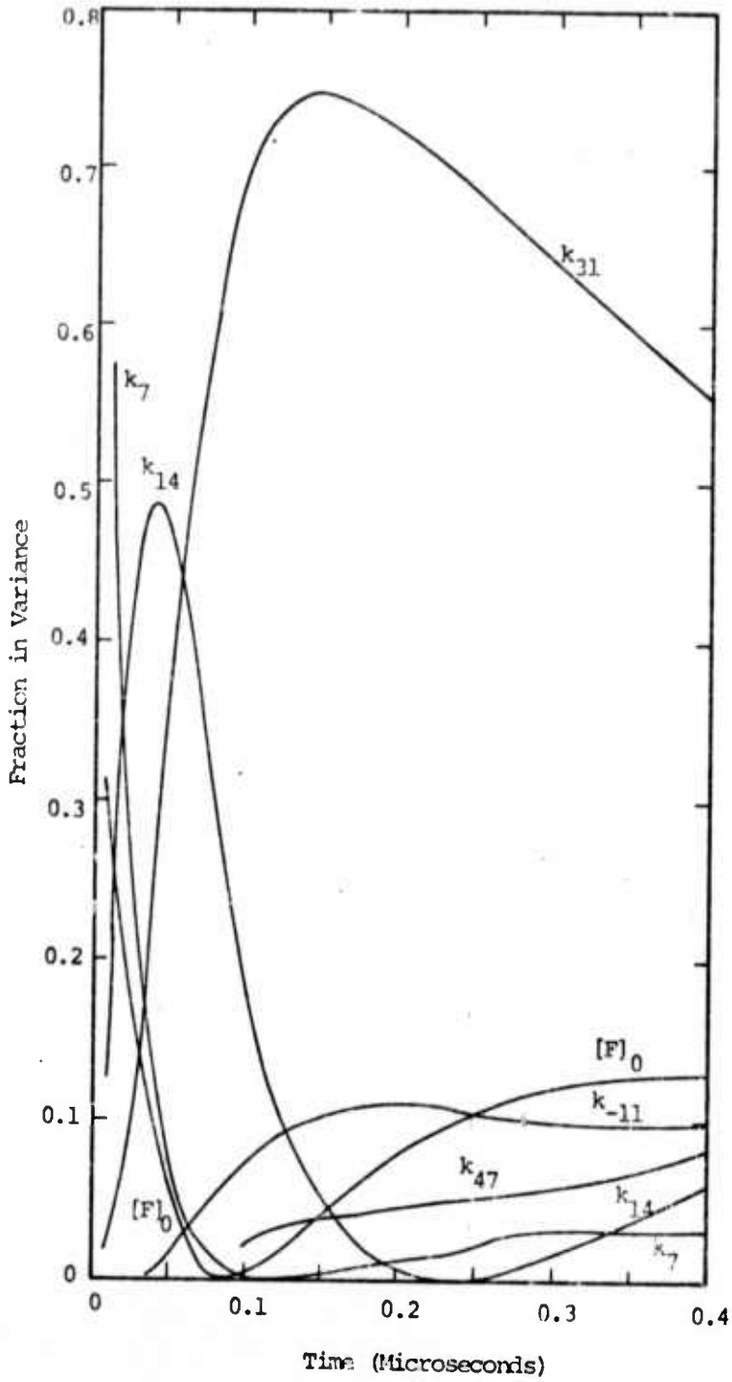

Figure 14. Variance spectrum for the zero power gain of the v = 3 → 2 band of HF.

4.2.3.10 Variance Spectrum of the Zero Power Gain on the v = 4→3 Transition of HF

In Fig. 15 we display the variance spectrum for the zero power gain on the HF (v = 4→3) transition. Recalling the discussion in Section 4.2.3.5, concerning the population of the HF (v = 4) level, we should expect to see a large contribution to the variance spectrum due to reaction rate constant k_{-11}, and indeed this is seen in Fig. 15. This immediately indicates that very large coefficient of variation for this gain (see Fig. 5) is due, in large measure, to uncertainties in the reverse of reaction no. 11, i.e., $HF(4) + H \rightarrow F + H_2(0)$. As indicated previously, we will discuss this point further in Section V. It might be noted here, however, that Kerber, et al.,[7] in their study also computed that the gain for this transition would be very small – smaller even than for the HF (v = 5→4) or HF (v = 6→5) transitions. This was confirmed in our calculation (see Fig. 3). But the large coefficient of variation and the unique sensitivity to k_{-11} suggest that something is amiss in the model: The HF (v = 4) level population does not properly "fit" into a logical scheme. In Section 5 we shall discuss the resolution of this "paradox".

4.2.3.11 Variance Spectrum of the Zero Power Gain on the v = 5→4 Transition of HF

In Fig. 16 we display the variance spectrum for the zero power gain on the HF (v = 5→4) transition. Compared to Fig. 15, the role of k_{-11} is much reduced. In other respects, the curves for this transition are similar to those of the HF (v = 3→2) transition (Fig. 14), except that the small k_{47} contribution does not appear. Thus, the variance spectrum for this gain shows the k_{-11} "anomaly" of Fig. 10, although reduced in amount; but in other respects it is similar to that for the other gains discussed above.

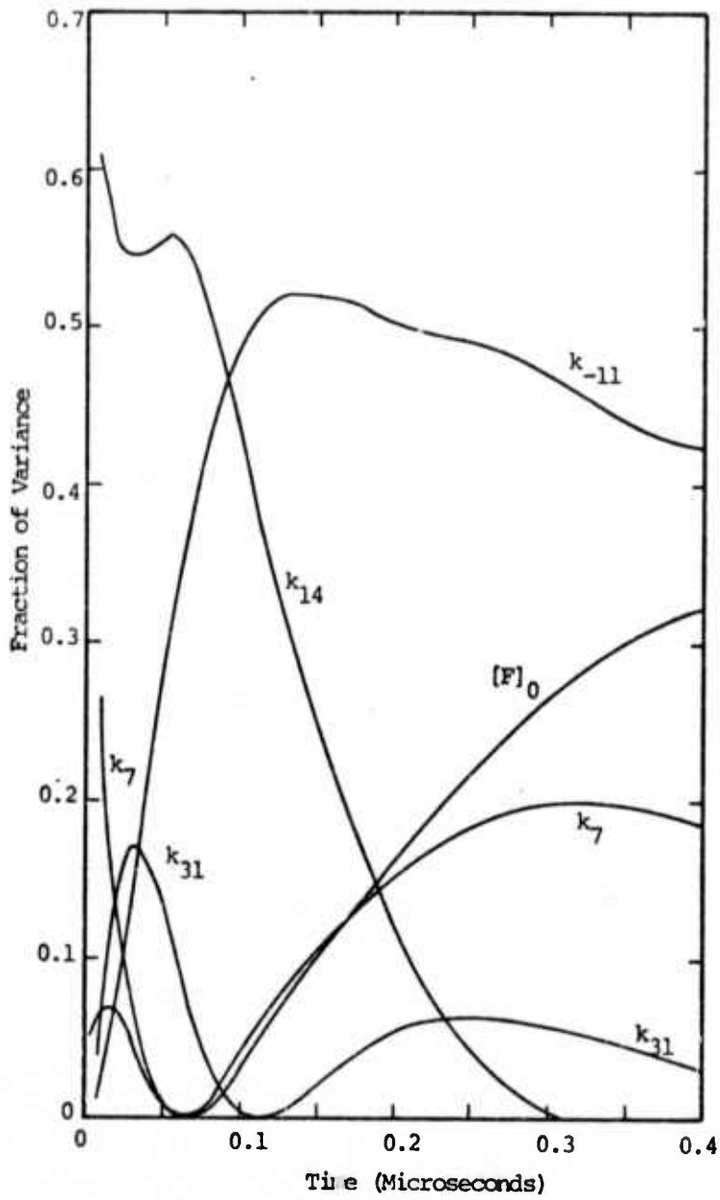

Figure 15. Variance spectrum for the zero power gain of the v = 4 → 3 band of HF.

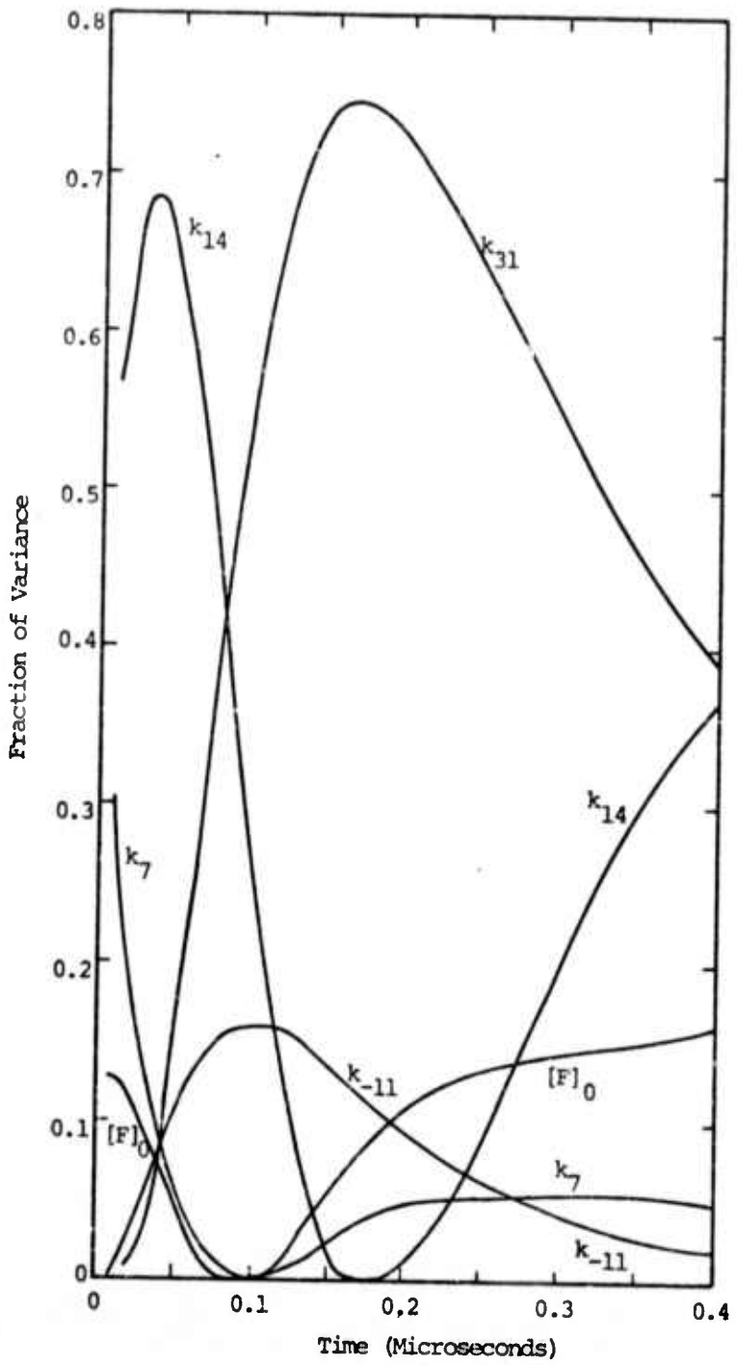

Figure 16. Variance spectrum for the zero power gain of the $v = 5 \rightarrow 4$ band of HF.

V. DISCUSSION OF RESULTS

In the preceeding section, we gave brief descriptions of the numerical results of the SAM analysis, as presented in sixteen figures. In this section, we will summarize these results of the analysis, and the conclusions which can be drawn therefrom.

The most obvious point is that most of the rate constant uncertainties have very little influence upon the predictions of the model. We see that the rate instants k_{-1}, k_2, k_3, k_{21}, k_{23}, k_{39}, k_{54}, and k_{60} contribute negligibly to the variance in the model's predictions, despite the factor-of-five inaccuracy in each of them. We will briefly review the chemical processes which correspond to this set of reactions.

5.1 UNIMPORTANT REACTIONS

Reaction No. 1: This is the collisional dissociation (reverse: recombination) of H_2 ($v = 0$) into H atoms. Clearly only the reverse (recombination) could be expected to be of significance, as the forward processes have a non-negligible rate only at temperatures of several thousand kelvins, well above the temperatures in the HF laser. But it turns out, as shown by the analysis, that the recombination process rate uncertainties do not importantly influence the model in the time range studied.

Reaction No. 2: This process plays the same role for F that Reaction No. 1 does for H; the reverse (recombination) process does not influence the model to any degree.

Reaction No. 3 (also Reactions 4, 5, and 6, because of the assumed proportionalities of rate constants): As with Reactions 1 and 2, only the reverse (recombination) can be significant; but here too the model is highly insensitive to the uncertainties in this rate constant.

It is worth noting that the previous paragraphs suggest that the model might not be significantly influenced by removing these six reactions altogether. Of course, if such were done, the model, because of the form of the remaining chemical equations, would not contain a sink for free radicals, which is not physically realistic. Nonetheless, once the bulk of the hydrogen and fluorine has reacted to produce HF (v = 0), it is clearly immaterial whether or not any residual free radicals (i.e., H and/or F) remain, since at that point no fuel remains to drive further lasing.

Reaction No. 21 (also No. 22, which is assumed to have the same rate): It is clear that these reactions can only be significant in the forward directions (deactivation of the excited vibrational states of H_2). This reaction could only influence HF populations and lasing indirectly, via reactions 65 to 68. But the latter processes are slow because of the mismatch in vibrational energies of H_2 and HF, and also because the excited state populations of H_2 are always small.

This suggests that the model might not be much affected if the six reactions, Nos. 21, 22, 65, 66, 67, and 68 were removed. It should be noted that Kerber, et al.[7] also noted the unimportance of these reactions (see Fig. 5 of their paper).

Reaction No. 23 (also Nos. 24 to 30 by the proportionality relations): These reactions, which deactivate excited states of HF by VT transfer to F atoms, are quite unimportant under the conditions considered here, and their rate uncertainties have almost no influence on the predictions of the model. The unimportance had previously been noted by Kerber, et al. (This statement may not apply at real times less than 0.1 μsec after initiation, where we have not carried out an analysis, and possibly this rate uncertainty impacts on the system prior to its attaining threshold.)

Reaction No. 39 (also Nos. 40 to 46 by the proportionality relations): The rate constants for these reactions appear to be too small for them to play an important role in deactivating the excited vibrational states of HF, despite the large amount of Ar in the system. It would appear that the model might well omit these reactions without much effect upon computational results.

Reaction No. 54 and 60 (also Nos. 55 to 59 and 61 to 64 because of the assumed proportionalities of rate constants): The rates for these processes are too small for them to affect the model, even with the possibility of a five-fold increase in all of the rates. Kerber, et al.[7] had previously noted this in their work.

The above paragraphs suggest that the model could be very much simplified with little effect upon its validity. As noted, most of the discussed reactions could be removed from the model. With their removal, the computing time per model run would be drastically reduced. It is conceivable that this reduction in computing time might be significant in the event that an attempt was made to construct a model of an HF chemical laser in nonsteady flow. For such a model, it is necessary to couple hydrodynamic equations to the chemical equations, and computing times become quite large, and strongly dependent upon the size of the chemical model. In such a case, the reduction in the chemical model suggested here could be valuable.

5.2 IMPORTANT REACTIONS

Only five rate constants, k_7, k_{-11}, k_{14}, k_{31}, and to a lesser extent k_{47}, are significant in that their uncertainties generate corresponding uncertainties in the predictions of the model. Thus, the corresponding reaction sets constitute the core of the model. Let us briefly review these reactions.

Reaction No. 7 (also Nos. 8, 9, 10 because of the proportionality relations): These are among the processes which lead to the formation of vibrationally excited HF, so that they directly impact on lasing.

Reaction No. 11 (also Nos. 12 and 13 because of the proportionality relations): Only the reverses (deactivations) are important here, and by definition these influence only the v = 4, 5, and 6 states of HF.

Reaction No. 14 (also Nos. 15 to 20 because of the proportionality relations): These are among the processes which lead to the formation of vibrationally excited HF, so that they directly impact on lasing.

Reaction No. 31 (also Nos. 32 to 38 because of the proportionality relations): These are the principal reactions whereby deactivation of excited HF molecules occurs. The rates for these processes are such that they are the dominant deactivation mechanism, almost to the exclusion of other deactivation processes.

Reaction No. 47 (also Nos. 48 to 53 because of the proportionality relations): This process (vibrational exchange between excited states of HF) has a small contribution to the variance spectra for the $v = 1 \rightarrow 0$ and $v = 3 \rightarrow 2$ bands of HF, but otherwise no influence. Because the effect is small, we have not examined it. The role of these reactions appears difficult to explain in detail. It, however, might be prudent to retain these reactions if a simplified model were to be constructed.

At early times the reactions of the "important" sets which lead to HF ($v > 0$) formation dominate uncertainties; at late times those which lead to HF ($v > 0$) deactivation dominate uncertainty. Except for the limited appearance of reaction no. 11, the early time reactions are nos. 7 and 14, the late

time reaction is only no. 39. Thus as a qualitative summary, we may state that the HF laser basically is governed by three chemical reactions:

(1) $F + H_2(O) \rightarrow HF(v) + H$

(2) $H + F_2 \rightarrow HF(v) + F$

(3) $HF(v) + HF(v') \rightarrow HF(v-1) + HF(v')$

Clearly also important is the initial concentration of F atoms, which has two impacts: One on the early time kinetics, and a second one, on the late time thermal history, since the initial F atom concentration fixes the internal energy of the system.

Except for the $v = 4 \rightarrow 3$ and $v = 5 \rightarrow 4$ gains, and the populations of the $v = 4$ and $v = 5$ levels of HF, the preceeding paragraph would appear to completely summarize the conclusions of the SAM analysis of this system, it being realized that it then follows that better model predictions will be dependent upon better rate data for the three important reactions.

The role of Reaction No. 11 is peculiar, and deserves specific comment.

As noted previously, reactions 11, 12 and 13 are such that only their reverses effectively occur; these reverses serve as an alternate to reactions 31-38 in deactivating HF(v). At the same time, reactions 3 to 10, functioning in reverse, deactivate HF(v) for $v = 1$, 2, and 3. Thus, there are in the model six deactivation reactions of the form

$$HF(v) + H \rightarrow H_2(0) + F$$

However, the model takes the temperature dependence of these reverse processes as being quite different. For $v = 4$, 5, 6 the temperature dependence is that stated in Table I, i.e., $k_{-7-v} = 10^{12}\ T^{0.67}\ cm^3\ mole^{-1}\ sec^{-1}$. For $v = 1$, 2, 3, the rates must be indirectly inferred via the equilibrium relations

$$k_{-n} = k_n / K_{EQ,n}$$

where $K_{EQ,n}$ is the equilibrium constant. The latter can be obtained from a thermodynamic analysis of the excited vibrational states of HF, the ground vibrational state of H_2 (which is virtually identical thermodynamically with an equilibrium distribution of the vibrational states of H_2), and the free atoms H and F. The results of such an analysis give complicated expressions for the deactivation rates of reactions 7 to 10, which are roughly of the form

$$k_{-n} = A_n T^{0.360} \exp(-B_n/T) ,$$

where A_n and B_n are approximately temperature independent. These expressions are completely different both in form and value (as a function of temperature) from the expression used for k_{-11}, k_{-12}, and k_{-13}. They also display strong dependence upon the value of v, whereas k_{-11}, k_{-12}, k_{-13} are independent of v.

Physically, we should expect the reaction of HF(v) with H atoms to vary in a consistent fashion as a function of v. In using, in effect, two different expressions for the rates of these processes, the model does not allow for such a consistent variation. The question then arises: Which of the two forms, i.e., the implied reverse of k_7, or k_{-11}, is more likely correct?

The answer can be surmised from the analysis of Cohen.[9] His work clearly shows that the value for k_7, based upon direct experimental work, is more reliable than that for k_{-11}, which is only indirectly inferred. He, in fact, suggests a quite different rate constant expression for k_{-11}. This latter expression was used by Suchard, et al.[10] in their further simulation work on the HF laser. Unfortunately, the computer calculations of Suchard, et al. differ from their experiments,

possibly for reasons such as parasitic oscillations, which are not included in the model. Thus even the revised rate expression of Suchard, et al.[10] is of uncertain validity. It would be desirable to repeat our analysis using Suchard's revised rate expression for k_{-11}, but we have not yet had an opportunity to do so.

In any event, we can see from Cohen's analysis that the rate expression for k_{-11}, as used in this work, is inferior to the rate expression used for k_7. This immediately explains the anomalously high variance in the gain computed for the v = 4→3 transition. We can conclude that this gain (and to a lesser extent the gain in the v = 5→4 transition), because of its particular sensitivity to the expression for k_{-11}, and because of incorrectness of the latter, is not predicted well by the model. As a corollary, we can also suggest the paradox of low gain on the computed v = 4→3 transition is an artifact of the model, obtained because of the incorrect rate constant used for reaction k_{-11}. It is our conjecture that the gain on the v = 4→3 will be found to be much higher than that predicted here, when a better value becomes available for the rate constant k_{-11}.

VI. CONCLUSIONS

The analysis of the HF laser presented above is a first effort at applying the SAM methodology to lasers. It clearly indicates which reactions are important and which are not, as discussed in the previous section. The indications provided therein are peculiar to the time range and zero power conditions under which the analysis was carried out. It would be worthwhile to extend this analysis to the case of finite power to check whether or not different reactions become significant at finite power levels. At the same time, it would be worthwhile to use Cohen's[9] revised expression for k_{-11}; and it also would be worth verifying whether the larger reaction set used by Suchard, et al.[10] leads to any new conclusions.

Not yet addressed is the question of the influence of the importance of the proportionalities assumed between sets of rate constants, as in Table I. It should be clear from Sections IV and V that the only proportionalities which can be important are those for (a) Eqs. (7) to (10); (b) for Eqs. (11) to (13); (c) for Eqs. (14) to (20); (d) for Eqs. (31) to (38). However, these proportionalities are likely to be very important, and can be expected to impact drastically upon the distribution of power among the transitions when the system operates at nonzero power. A SAM analysis of these proportionalities should yield useful information.

The present study does not consider the time prior to 0.1 μsec after initiation, and therefore, does not consider time-to-threshold. Extension of the SAM analysis to this short time range would be straightforward, and conceivably could lead to a modified assessment of the relative importance of the various reactions. The present study also does not consider nonzero initial concentrations of HF, which as noted earlier, can be expected to have an effect upon both the

predictions of the model and upon real laser performance. It would be of particular interest to treat the initial HF concentration as a parameter, so as to see how numerical uncertainties in its value might affect performance.

On a more mathematical level, we previously indicated that our computer program differs from the program used previously[7,10] in that it employs an analytic matrix inversion scheme rather than numerical inversion. This inversion problem only arises when the system is lasing, and time has not yet allowed us to compute the lasing case. Therefore, our inversion porcess is in reality untested. It is our belief that analytic inversion may have the advantage of allowing faster computing, but actual calculations would be needed to verify this. If true, this analytic method could be favorably employed in laser models other than the HF model. Work on this analytic inversion method is warranted.

Finally, we should consider the application of the SAM method to lasers other than the HF laser. Laser models in general are complex and multiparametric. Tools for understanding the models therefore are useful and SAM is one such tool. As with the model studied here, it could, with other models, determine the relative importance of the parameter uncertainties. These uncertainties need not be only those in the rate constants, but can also include zero time species concentrations (such as that for F atoms here), geometrical parameters of the systems, diffusion constants in flow systems, pumping efficiency, loss mechanisms, and others. Because of their great practical importance, early study of CO_2 laser models is warranted. Application of the SAM technique should be able to provide useful insights as to the important characteristics of such systems.

REFERENCES

1. H. Weyl, "Mean Motion," American Journal of Mathematics, Vol. 60, pp. 889-896, 1938.

2. R. I. Cukier, C. M. Fortuin, K. E. Shuler, A. G. Petschek and J. H. Schaibly, "Study of the Sensitivity of Coupled Reaction Systems to Uncertainties in the Rate Coefficients. I. Theory," J. Chem. Phys., 59, p. 3873, 1973.

3. J. H. Schaibly and K. E. Shuler, "Study of the Sensitivity of Coupled Reaction Systems to Uncertainties in the Rate Coefficients. II. Applications," J. Chem. Phys., 59, p. 3879, 1973.

4. H. B. Levine and J. H. Schaibly, "Sensitivity of Fireball Chemistry Calculations to Uncertainties in the Rate Coefficients (U)," Systems, Science and Software Report No. SSS-CR-74-2051, February 1974. The latter report is classified "Secret." Requests for copies must be submitted to the cognizant project officer: Dr. John Dardis, Office of Naval Research, Department of the Navy, 800 North Quincy Street, Arlington, VA 22217; Telephone (202) 692-4219.

5. R. V. Churchill, "Fourier Series and Boundary Value Problems," McGraw-Hill, New York, pp. 43, 85, 86, 1941.

6. R. B. Blackman and J. W. Tukey, "The Measurement of Power Spectra," Dover Publications, New York, 1958.

7. R. L. Kerber, G. Emanuel, and J. S. Whittier, "Computer Modeling and Parametric Study for a Pulsed H_2+ F_2 Laser," Applied Optics, 11, p. 1112, 1972.

8. G. Emanuel, N. Cohen, and T. A. Jacobs, "Theoretical Performance of an HF Chemical CW Laser," Aerospace Corporation Report No. TR-0172(2776)-2, February 15, 1972.

9. N. Cohen, "A Review of Rate Coefficients for Reactions in the H_2-F_2 Laser Systems," Aerospace Corporation Report No. TR-0172(2779)-2, 1972.

10. S. N. Suchard, R. L. Kerber, G. Emanuel, and J. S. Whittier, "Effect of H_2 Pressure on Pulsed H_2+F_2 Laser: Experiment and Theory," Journal of Chemical Physics, 57, p. 5066, 1972.

11. G. Emanuel, "Analytical Model for a Continuous Chemical Laser," Journal of Quantum Spectroscopy and Radiative Transfer, 11, p. 1481, 1971.

12. E. B. Turner, G. Emanuel and R. L. Wilkins, "The Nest Chemistry Computer Program," Aerospace Corporation Report No. TR-0059(6240-20)-1, Vol. I., July 30, 1970.

13. G. Emanuel, W. D. Adams and E. B. Turner, "Resale - 1: A Chemical Laser Computer Program," Aerospace Corporation Report TR-0172(2776)-1, March 15, 1972.

14. E. B. Turner, W. D. Adams, and G. Emanuel, "Numerical Formulation for Constant-Gain Chemical Laser Calculations," Journal of Computational Physics, 11, p. 15, 1973.

DISTRIBUTION LIST

DEPARTMENT OF DEFENSE

Director
Advanced Research Projects Agency
2 cy ATTN: Program Management

Director
Defense Documentation Center
12 cy ATTN: DODAAD Code S47031

Commander
Defense Contract Administration

DEPARTMENT OF THE NAVY

Office of Naval Research
3 cy ATTN: Dr. J. G. Dardis
Physics Program
Physical Sciences Division

Office of Naval Research
ATTN: Mr. R. H. Register
Contracting Office

Director
Naval Research Laboratory
6 cy ATTN: Code 2629

Director
Naval Research Laboratory
6 cy ATTN: Code 2627